

Article

Targeting Acidic Mammalian Chitinase is Effective in Animal Model of Asthma

Marzena Mazur, Jacek Olczak, Sylwia Olejniczak, Robert Koralewski, Wojciech Czestkowski, Anna Jedrzejczak, Jakub Golab, Karolina Dzwonek, Barbara Dymek, Piotr L. Sklepkiwicz, Agnieszka Zagodzón, Tom Noonan, Keyvan Mahboubi, Bruce Conway, Ryan Sheeler, Paul Beckett, William M. Hungerford, Alberto D. Podjarny, Andre Mitschler, Alexandra Cousido-Siah, Firas Fadel, and Adam Golebiowski

J. Med. Chem., **Just Accepted Manuscript** • DOI: 10.1021/acs.jmedchem.7b01051 • Publication Date (Web): 28 Dec 2017

Downloaded from <http://pubs.acs.org> on December 29, 2017

Just Accepted

“Just Accepted” manuscripts have been peer-reviewed and accepted for publication. They are posted online prior to technical editing, formatting for publication and author proofing. The American Chemical Society provides “Just Accepted” as a free service to the research community to expedite the dissemination of scientific material as soon as possible after acceptance. “Just Accepted” manuscripts appear in full in PDF format accompanied by an HTML abstract. “Just Accepted” manuscripts have been fully peer reviewed, but should not be considered the official version of record. They are accessible to all readers and citable by the Digital Object Identifier (DOI®). “Just Accepted” is an optional service offered to authors. Therefore, the “Just Accepted” Web site may not include all articles that will be published in the journal. After a manuscript is technically edited and formatted, it will be removed from the “Just Accepted” Web site and published as an ASAP article. Note that technical editing may introduce minor changes to the manuscript text and/or graphics which could affect content, and all legal disclaimers and ethical guidelines that apply to the journal pertain. ACS cannot be held responsible for errors or consequences arising from the use of information contained in these “Just Accepted” manuscripts.

Targeting Acidic Mammalian Chitinase is Effective in Animal Model of Asthma

Authors:

Marzena Mazur,[†] Jacek Olczak,[†] Sylwia Olejniczak,[†] Robert Koralewski,[†] Wojciech Czestkowski,[†] Anna Jedrzejczak,^{†,¶} Jakub Golab,^{†,□} Karolina Dzwonek,[†] Barbara Dymek,[†] Piotr L. Sklepkiewicz,[†] Agnieszka Zagozdzon,[†] Tom Noonan,[†] Keyvan Mahboubi,[†] Bruce Conway,[†] Ryan Sheeler,[†] Paul Beckett,^{‡,#} William M. Hungerford,^{‡,//} Alberto Podjarny,[§] Andre Mitschler,[§] Alexandra Cousido-Siah,[§] Firas Fadel,^{§, &} Adam Golebiowski^{*,†}

[†] OncoArendi Therapeutics SA, Żwirki i Wigury 101, 02-089 Warsaw, Poland

[□] Department of Immunology, Medical University of Warsaw, 1A Banacha Str., 02-097 Warsaw, Poland

[‡] The Institute for Pharmaceutical Discovery, Business Drive 23, 06-405, Branford, CT, USA

[§] Department of Integrative Biology, IGBMC, CNRS, INSERM, Université de Strasbourg, 1 rue Laurent Fries, 67404 Illkirch, France

Abstract. This article highlights our work toward the identification of a potent, selective, and efficacious acidic mammalian chitinase (AMCase) inhibitor. Rational design, guided by X-ray analysis of several inhibitors bound to human chitotriosidase (hCHIT1) led to the identification of compound **7f** as a highly potent, AMCase inhibitor (IC₅₀ values of 14 and 19 nM against human and mouse enzyme, respectively) and selective (>150x against mCHIT1) with very good PK properties. This compound dosed once daily at 30 mg/kg p.o. showed significant anti-inflammatory efficacy in HDM-induced allergic airway inflammation in mice, reducing inflammatory cell influx in the BALF and total IgE concentration in plasma, which correlated with decrease of chitinolytic activity. Therapeutic efficacy of compound **7f** in the clinically relevant aeroallergen-induced acute asthma model in mice provides a rationale for developing AMCase inhibitor for the treatment of asthma.

Introduction:

Allergic asthma, which affects nearly 300 million people, is a chronic inflammatory disease, dominated by type 2 immunity. Immune responses to inhaled allergens include eosinophilic inflammation, goblet cell metaplasia, mucus oversecretion, subepithelial fibrosis and airway hypersensitivity. Nearly 85% of asthmatics are responsive to chitin-containing house dust mite (HDM) allergens and animal models of asthma frequently use HDM extract to induce allergic airway inflammation. Although mammals do not produce chitin, the second most abundant polymer in nature, they express two enzymes digesting it: acidic mammalian chitinase (AMCase) and chitotriosidase (CHIT1), as well as several chitin-binding proteins, such as YKL-40 (BRP-39 in mice), YM1, YM2, or oviductin.¹ Among true chitinases, AMCase has been shown to be produced during type 2 inflammatory responses in several diseases, both in murine asthma models^{2,3} and in allergic patients.^{2,4} Early studies have shown that AMCase neutralization with monoclonal antibodies², its genetic ablation with shRNA⁷ or inhibition of its enzymatic activity with the pseudotrisaccharide natural products allosamidin or demethylallosamidin^{2,8} results in diminution of IL-13-mediated allergic inflammation or ovalbumin (OVA)-induced allergy in the lungs. Several potent natural product chitinase inhibitors have been identified, including the mentioned above pseudosaccharides allosamidin⁹ and demethylallosamidin, the cyclic peptides argadin and argifin,¹⁰ and several xanthine derivatives,¹¹ including theophylline, caffeine, and pentoxifylline (Figure 1).

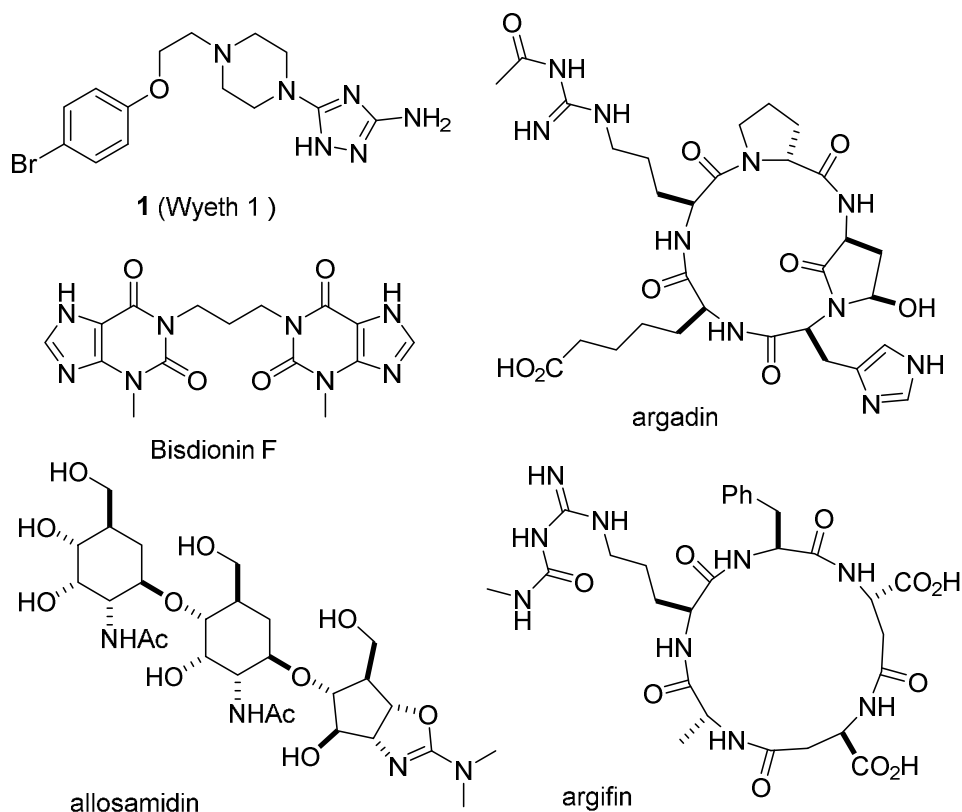


Figure 1. Examples of AMCase and CHIT1 inhibitors

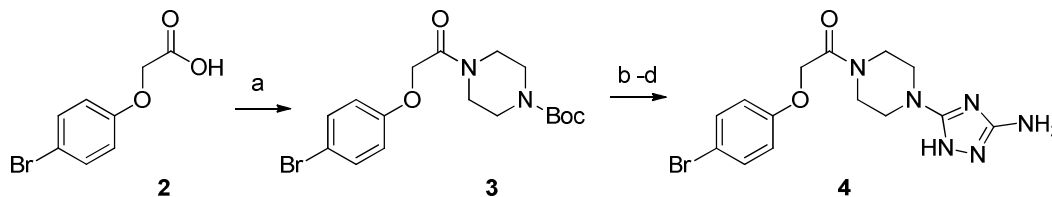
The therapeutic potential or use of these compounds as biological tools is limited due to their sizes, complex chemistries, limited availabilities, and poor pharmacokinetic profiles in addition to pleiotropic modes of action, especially for the xanthine derivatives. Bisdionin F, a rationally designed and selective (vs CHIT1) AMCase inhibitor alleviated the primary features of allergic inflammation including eosinophilia in the OVA model in mice.¹² Wyeth developed a moderately active, dual inhibitor (compound **1**) of AMCase and CHIT1¹³. Graphene oxide was shown to inhibit enzymatic activity of AMCase and to attenuate Th2-type immune responses in a murine model of asthma¹⁴. Conversely, some studies have cast doubt as to whether AMCase inhibition would be effective in asthma treatment. Mice congenitally lacking AMCase (constitutive CHIA, whole-body knock-out animals) developed normal airway inflammation in HDM or OVA-induced allergy models and allosamidin as well as inhibitor **1** failed to inhibit airway inflammation in this study.¹⁵ In other reports, AMCase overexpression resulted in ameliorated type 2 response induced by chitin¹⁶ and transgenic mice overexpressing enzymatically inactive AMCase were reported to develop increased allergic airway inflammation¹⁷.

1
2
3 However, congenital defects in AMCcase might not represent a suitable model for studying the role of
4 this enzyme in acute responses induced in adult animals. Moreover, no data on the pharmacokinetic
5 properties of the AMCcase inhibitors used in this study was provided.¹⁵ Studies in mice overexpressing
6 AMCcase focused on the response induced by artificial chitin polymers covalently attached to
7 polystyrene beads.¹⁶ Finally, enzymatically deficient AMCcase¹⁷ was proven to bind a chitin
8 resembling this protein to BRP-39, which similarly to its human homolog YKL-40 is induced in
9 aeroallergen asthma models¹⁸ and in human asthma patients^{19,20}, respectively. Therefore, the
10 contrasting observations on the role of AMCcase in animal asthma models require development of
11 more in vitro active compounds with a pharmacokinetic profile suitable for in vivo studies. To this
12 end, we have developed a new series of compounds with excellent in vitro activity, selectivity versus
13 CHIT1 and suitable PK properties allowing oral administration once daily. Finally, we demonstrated
14 strong anti-inflammatory effects of these compounds in an HDM-induced airway inflammation model
15 in mice that reveal AMCcase to be an appropriate therapeutic target in asthma.
16
17
18
19
20
21
22
23
24
25
26
27
28
29

30 SYNTHETIC CHEMISTRY

31
32 Molecule **1** has been reported by Cole and co-workers.¹³ The synthesis of an amide analog **4** started by
33 acylation of 1-(tert-butoxycarbonyl)piperazine to give intermediate **3** (Scheme 1). Unmasking the
34 second amine group and installation of 2-aminotriazole ring, using modified previously reported
35 synthesis²¹ led to molecule **4**.
36
37
38
39

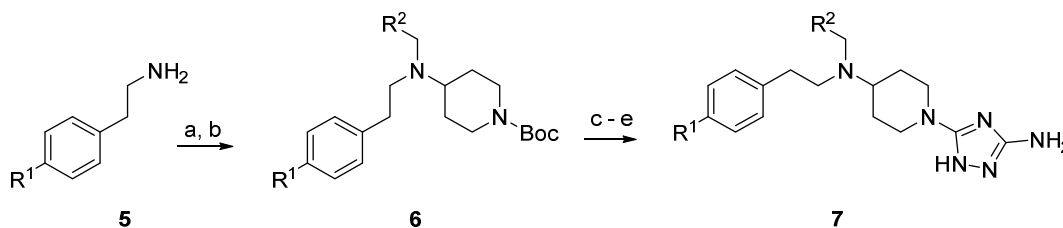
40 Scheme 1. Preparation of amide **4**^a



50 ^aReagents and conditions: (a) 1-(tert-Butoxycarbonyl)piperazine, TBTU, DIPEA, DCM, rt; (b) HCl,
51 EtOAc, rt; (c) S,S'-Dimethyl N-Cyanodithioiminocarbonate, K₂CO₃, MeCN, 82°C; (d) Hydrazine,
52 MeCN, 82°C.
53
54
55
56
57
58
59
60

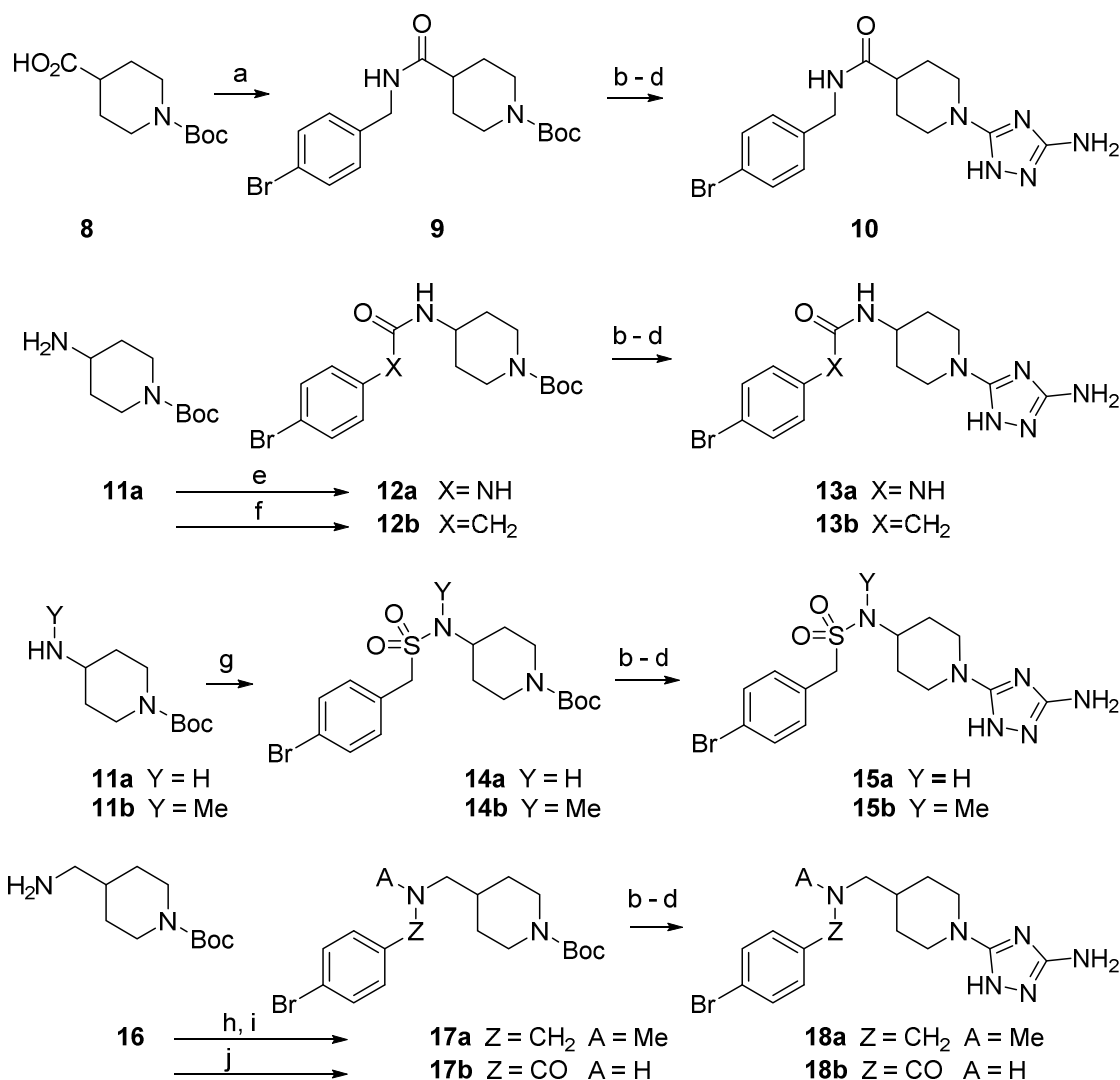
Most of N-alkyl compounds (**7**) were made using general procedure (Scheme 2). Reductive amination of respective phenethylamine **5** with N-Boc-4-piperidone, followed by the second reductive amination using appropriate aldehyde led to intermediate **6**. Amino group deprotection followed by installation of 2-amino-triazole ring system gave final compound **7**.

Scheme 2. General synthesis of analogs **7**^a



^aReagents and conditions: (a) N-Boc-4-piperidone, $\text{NaBH}(\text{OAc})_3$, DCE, rt; (b) $R^2\text{CHO}$, $\text{NaBH}(\text{OAc})_3$, DCE, rt; (c) HCl, EtOAc, rt; (d) S,S'-Dimethyl N-Cyanodithioiminocarbonate, K_2CO_3 , MeCN, 82°C ; (e) Hydrazine, MeCN, 82°C .

An amide **10** was prepared in the straightforward 4-bromobenzylamine acylation, Boc-deprotection and 2-aminotriazole ring installation sequence. Urea analog **13a** as well as an amide **13b** was made using similar synthetic sequence, starting from monoprotected 4-aminopiperidine **11a**. The same starting material as well as its N-methyl analog **11b** was used to make sulfonamide **15a** and its N-methyl derivative **15b**. Piperidine **16** served as a substrate to make amine **18a** and an amide **18b** (Scheme 3).

Scheme 3. Synthesis of compounds: **10**, **13a-b**, **15a-b**, **18a-b**^a

^aReagents and conditions: (a) 4-Bromobenzylamine, TBTU, DIPEA, CH₂Cl₂, rt; (b) HCl, EtOAc, rt; (c) S,S'-Dimethyl N-Cyanodithioiminocarbonate, K₂CO₃, MeCN, 82°C; (d) Hydrazine, MeCN, 82°C; (e) 4-bromoaniline, DIPEA, COCl₂, Toluene, 0°C to rt; (f) 4-Bromophenylacetic acid, TBTU, DIPEA, CH₂Cl₂, rt; (g) 4-Bromobenzylsulfonyl chloride, DIPEA, CH₂Cl₂, rt; (h) 4-Bromobenzaldehyde, NaBH(OAc)₃, DCE, rt; (i) HCHO, NaBH(OAc)₃, DCE, rt; (j) 4-Bromobenzoic acid, TBTU, DIPEA, CH₂Cl₂, rt.

RESULTS AND DISCUSSION

After reviewing the known chitinase inhibitors we decided to focus on the literature reported compound **1**.¹³ It is a relatively weak and non-selective AMCase inhibitor [human AMCase (hAMCase) IC₅₀ 5.5 μM; human CHIT1 (hCHIT1) IC₅₀ 6.8 μM], but its good drug-like profile and analysis of crystallographic data (PDB ID: 3RM4) indicated that it could be further optimized.

Table 1. SAR results of early analogs of inhibitor 1^a

Compd #	hAMCase (IC ₅₀ nM)	hCHIT1 (IC ₅₀ nM)	mAMCase (IC ₅₀ nM)	mCHIT1 (IC ₅₀ nM)
1	5450±1032	6755±134	2095±559	19800±2970
4	12250±778	>100,000	1355±403	>100,000
10	>100,000	>100,000	>100,000	>100,000
13a	>100,000	>100,000	>100,000	>100,000
13b	>100,000	>100,000	>100,000	>100,000
15a	3325±304	>100,000	573±126	>100,000
15b	>100,000	>100,000	>100,000	>100,000
18a	>100,000	>100,000	>100,000	>100,000
18b	>100,000	23100±4100	>100,000	>100,000

^aIC₅₀ data of each compound were determined in 2–3 independent assays, and mean IC₅₀ ± SD values are shown in the table. Compd, abbreviation of compound; SD, standard deviation.

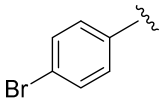
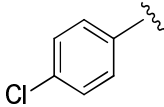
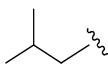
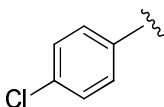
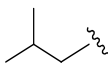
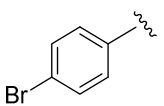
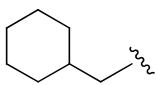
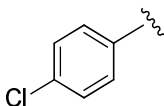
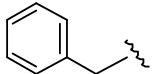
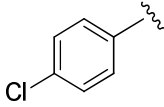
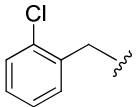
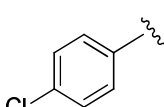
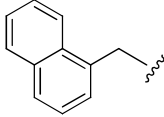
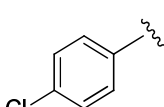
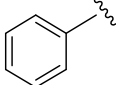
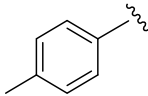
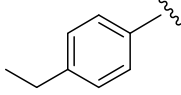
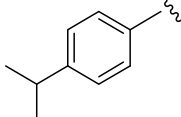
First attempts to identify key interactions and optimize activity were not very successful. Modification of the central nitrogen atom, shifting its position, changing its character (e.g. from the basic tertiary amine to an amide), generally led to inactive compounds with the major exception of 4-amino-piperidine analogs: compounds **7a-s** and **15a**.

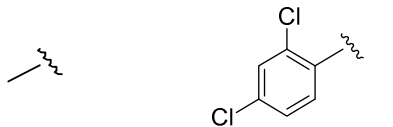
An X-ray crystallography approach was used to understand, at the atomic level, the mechanism behind the increased activity displayed by both compounds **7a** and **7b** towards hAMCase and hCHIT1 enzymes. The hCHIT1-compound **7a** complex structure was solved to 1.35 Å resolution by molecular replacement (Fig. 2A), using the hCHIT1 native structure (PDB ID: 4WJX)²² as the search model. As

hAMCase and hCHIT1 have a similar active site, the X-ray structure obtained allows us to propose the binding pattern of compound **7a** for both proteins. We next compared the binding patterns of compounds **1** and **7a** by superimposing the new hCHIT1-compound **7a** structure to the previously reported AMCase-compound **1** structure (PDB ID: 3RM4) (Fig 2B). Our comparison indicates that by replacing the compound **1** piperazine core to a 4-amino-piperidine ring in compounds **7a** and **7b**, the accommodation of these two latter within the active site of hCHIT1 is improved and a similar mechanism could be proposed for hAMCase. Indeed, we noticed that our new lead compound **7a** entered ~1 Å deeper in hCHIT1's pocket as compared to compound **1**. Interestingly, this difference is crucial for enabling Asp213 to establish a strong H-bond of 2.80 Å with the nitrogen of the central 4-aminopiperidine ring. In contrast to compound **1**, the Asp213 interacted with its piperazine central nitrogen through a weak H-bond of 3.7 Å (Fig 2 2B, C). Accordingly, we reasoned that strengthening the interaction between Asp213 and the core of the screened compounds is a key factor to increase the potency of compound **7a** towards both hAMCase and hCHIT1.

Table 2. SAR of analogs 7^a

Compd #	R1	R2	hAMCase (IC ₅₀ nM)	hCHIT1 (IC ₅₀ nM)	mAMCase (IC ₅₀ nM)	mCHIT1 (IC ₅₀ nM)
7a			348 ±21	175±7.1	108±17	2700±85
7b			660±8	389±12.7	245±35	7470±1160
7c			182±18	385±40	95±3	7080±396

1							
2							
3							
4	7d			73±4	105±36	36±12	2715±190
5							
6							
7							
8	7e			134±8	945±21	185±43	15650±636
9							
10							
11							
12	7f			14.2±1.0	232±48	18.8±0.4	2955±50
13							
14							
15							
16							
17	7g			8.7±1.3	123±47	8.0±2.5	1269±54
18							
19							
20							
21	7h			8.7±1.0	123±25	8.0±2.9	2025±205
22							
23							
24							
25	7i			5.4±1.6	163±70	11.2±2.1	1508±2.8
26							
27							
28							
29							
30	7j			3.5±0.4	149±77	9.7±3.5	2585±261
31							
32							
33							
34	7k			3.4±1.1	36±9	6.2±0.4	573±60
35							
36							
37							
38							
39	7l			18450±3040	>100,000	24400±	>100,000
40							
41							
42							
43	7m			1111±182	1525±304	544±13	12550±2192
44							
45							
46							
47	7n			970±34	1011±154	1430±382	7121±397
48							
49							
50							
51							
52							
53	7o			4137±1760	1175±205	1288±738	6965±92
54							
55							
56							
57							
58							
59							
60							

1						
2						
3						
4						
5	7p		1545±177	765±149	1735±445	3070±438
6						
7						
8						
9						
10	7r		13200±1980	4160±56	7330±57	>100,000
11						
12						
13						
14						
15						
16	7s		2025±163	2255±120	333±31	47600±3677
17						
18						
19						
20						

^aIC₅₀ data of each compound were determined in 2–3 independent assays, and mean IC₅₀ ± SD values are shown in the table. Compd, abbreviation of compound; SD, standard deviation.

This observation is in agreement with the IC₅₀ values showed in Table 1. All other placements of central nitrogen atom as well as its acylation/urea formation as in compounds **4**, **10**, **13a**, **13b**, **18a** and **18b** led to very weak inhibitors or inactive molecules, presumably because of breaking critical interaction of central nitrogen atom with Asp213 of the enzyme. The only exception in this series was sulfonamide **15a**, capable of forming hydrogen bond between Asp213 and hydrogen atom of the NH-sulfonamide group. N-Alkylation of sulfonamide nitrogen atom (i.e. formation of compound **15b**) gave also an inactive hAMCase/hCHIT1 molecule, further verifying critical interactions with Asp213. It is worth noting the AMCase/CHIT1 selectivity of molecule **15a**, although its activity was still moderate. A second important distinctive point revealed by the hCHIT1-compound **7a** co-crystal structure refers to the remarkable inversion of Trp99 which plays an important role in binding the chito-oligosaccharide substrate. Indeed, both hCHIT1 and hAMCase structures in complex with allosamidin, compound **1** (Fig 1, 2B, C) and other published ligands co-structures show a similar position of Trp99 in their native structures.¹¹⁻¹³ However, in our hCHIT1-compound **7a** co-structure, the Trp99 residue shows a 106° movement induced by a π-stacking interaction as the distance between the methyl group at the R1 position of the compound and the aromatic ring is 3.7 Å (Fig 2A, B, C). Moreover, this new Trp99 position induces a stacking interaction with the 4-amino-piperidine group

1
2
3 thus strengthening the binding with the compound. As the compound **1** does not have a R1 group,
4 the position of Trp99 adopts the native conformation and does not interact with the piperazine group
5 as the distance between them is 4.9 Å (Fig 2B, C). Thus, we can conclude that substituting the
6 piperazine ring with the 4-amino-piperidine, together with the addition of a new hydrophobic function
7 at the R1 position in compounds **7a** and **7b** strongly contribute to the new interaction of the
8 compounds with Trp99. We suggest that the recruitment of Trp99 plays an important role in the
9 improved potency of these compounds.
10

11 It is important to note that we observe a difference in binding of the aminotriazole group to the highly
12 conserved catalytic site of CHIT1. Indeed, while Asp138, Tyr27 and Tyr212 directly H-bond this
13 moiety of compound **7a**, the catalytic residue Glu140 interacts indirectly with the N of the
14 aminotriazole group via a water molecule (Fig. 3). Therefore, this water molecule gets stabilized by
15 establishing two strong H-bonds of 2.8 Å with Glu140 and with the N of the aminotriazole group.
16

17 Previous studies²² have shown that Asp138 can adopt a double conformation in the apo enzyme: one
18 linked to Asp136 and a second one oriented to Glu140. In the presence of compound **7a**, Asp138 is
19 oriented toward Asp136 through a low barrier H-bond (Fig. 3) and a water molecule mediating the
20 interaction between Glu140 and compound **7a** occupies the position of the carbonyl group in Asp138
21 second conformation thus forcing Asp138 to remain in its first conformation. In contrast, a direct
22 interaction is established between Glu140 and the N of the aminotriazole group of compound **1** and no
23 detectable water molecule is found in the pocket. This difference gives a structural mechanistic
24 explanation that could be one of the factors responsible for the increased potency seen in compound **7a**
25 vs. **1**. This structural information provided essential knowledge to further develop our compounds.
26
27
28
29
30
31
32
33
34
35
36
37
38
39
40
41
42
43
44
45
46
47
48
49
50
51
52
53
54
55
56
57
58
59
60

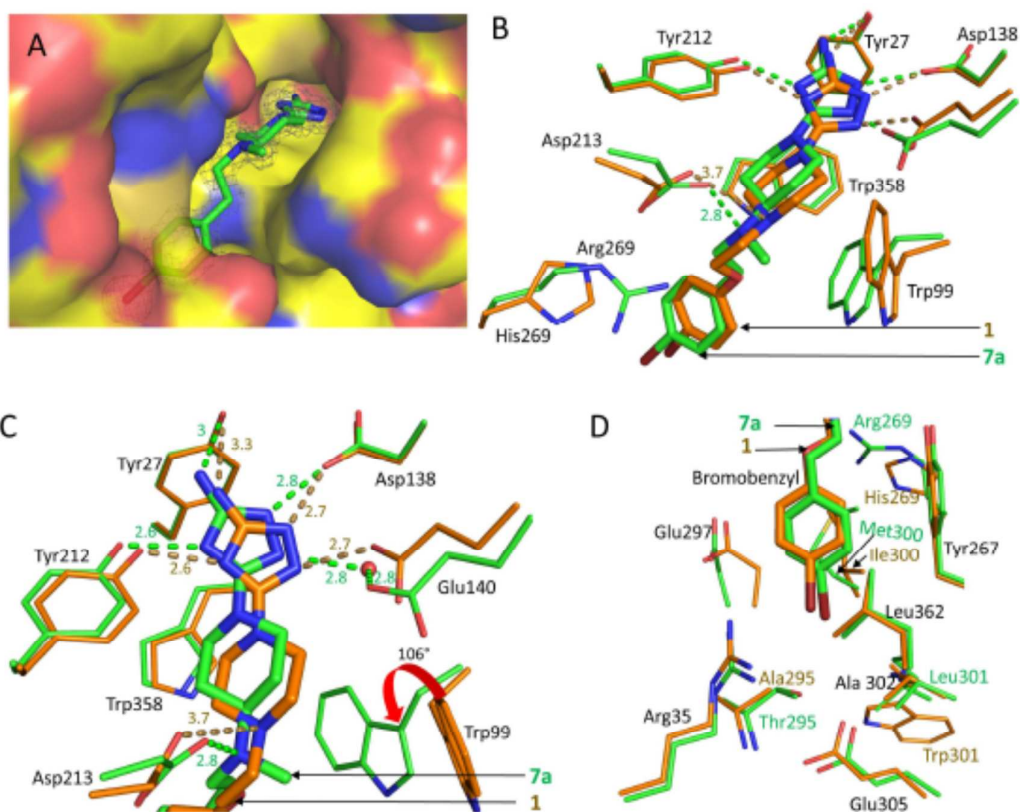


Figure 2 Structure of the hCHIT-compound **7a** complex and comparison to the hAMCase-compound **1** complex structure. A) contacts of compound **7a** represented as stick (green carbons) in the active site pocket of hCHIT1 represented as surface and colored according to charges. The 2mFo-Fc electron-density map (1σ cutoff) compound **1** is shown as a mesh colored in grey. B) Superimposition of the active site residues in hCHIT1 complexed to compound **7a** (stick model, carbons and distances colored in green) and the active site residues in hAMCase complexed to compound **1** (stick model, carbons and distances colored in orange). C) Zoomed superposition of compounds **7a** and **1** and key residues of hCHIT1 and hAMCase active site. The interaction between Glu140 residue in hCHIT1 and the N of the aminotriazole group is mediated by a water molecule (shown as a red sphere) while the interaction is direct in hAMCase-compound **1** complex. The Trp99 in hCHIT1 is inverted by 106° in hCHIT1-compound **7a** complex. D) Accommodation of R2 function (bromobenzyl moiety in compound **7a** and **1**) within the hydrophobic pocket of hCHIT1 and hAMCase).

To obtain an inhibitor selective for hAMCase, several compounds were generated by modifying substituents R1 and R2. Our *in vitro* assays revealed that compounds **7g** and **7i** display a 15- and 44-

fold selectivity against hAMCase as compared to hCHIT1, respectively. Therefore, we sought to investigate the structural basis that explains such high selectivity. For this, we have used the soaking method with the two identified hit compounds and solved their X-ray crystal co-structures in complex with hCHIT1 at 1.27 Å and 1.44 Å resolutions respectively. Both structures show that the main body of the two compounds binds similarly to compound **7a** in hCHIT1 catalytic groove (Fig. 3).

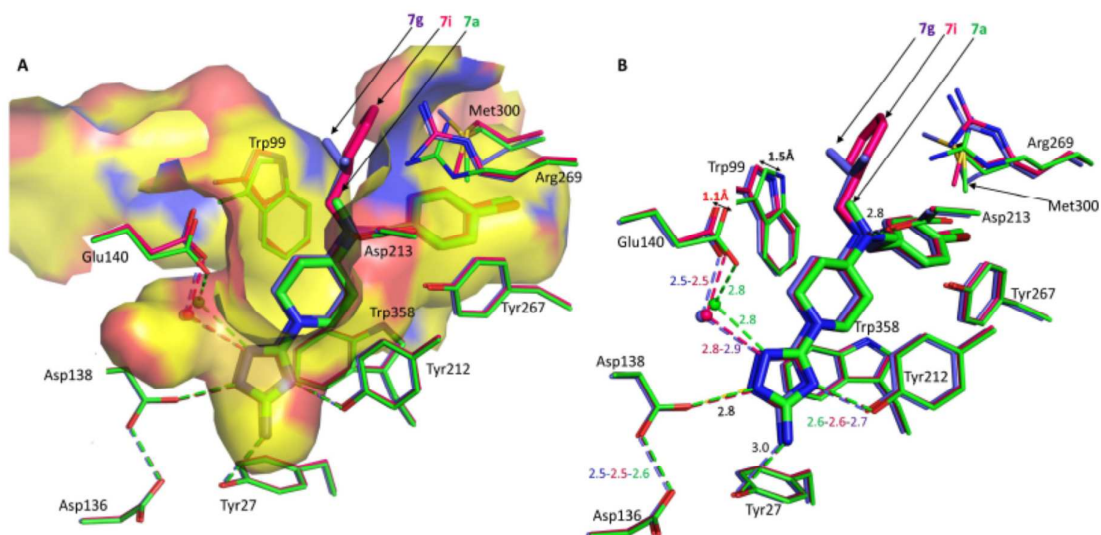


Figure 3. Superimposition of the active site region of the three complex structures hCHIT1-compound **7a**, **7i** and **7g**. Key residues are represented by lines with oxygen atoms in red, nitrogen atoms in dark blue, sulfur atoms in yellow. A) Active site pocket of hCHIT1 represented as surface and colored according to charges. In A) and B) compounds **7a**, **7i** and **7g** are represented in stick, carbons are colored in green, violet and magenta, respectively, chlorine atoms are colored in light green and bromide atoms in dark red. The water molecule mediating the interaction with the aminotriazole group is color coded according to the compound it interacts with. In B) the distance between atoms is color-coded according to the compound it interacts with.

The R2 which corresponds to bromobenzyl function in **7a** and **7g** is a chlorobenzyl in **7i**. This moiety in the three compounds occupies in the same way the hydrophobic pocket formed by Leu362, Ala302, Leu301, Met300, and Tyr267 residues with 1 Å shift to compound **1**. The presence of a phenyl function in R1 in compound **7i** shows a stacking contact with Met300 which should take place with Ile300 in hAMCase. The superposition of the three hCHIT1-ligands co-structures shows that the

1
2
3 position of the Trp99 dictated by the stacking is slightly deviated of (~ 1.5 Å) depending on the R1
4 fragment (Fig 3). This deviation of Trp99 seems to be accompanied by slight displacement (of ~ 1 Å)
5 of the key Glu140 residue and the water molecule involved in the Glu140-ligand interaction (Fig 3).
6
7 Consequently, this displacement appears to be crucial to reinforce the contact between Glu140 and the
8 water molecule. Thus, the distance of this H-bond shifts from 2.75 Å in the hCHIT1-compound **7a**
9 complex to a low barrier H-bond of 2.50 Å in the complexes hCHIT1-compound **7g** and **7i**
10 respectively (Fig. 3B). As the key residues involved in the interaction with compounds **7g** and **7i**
11 except Met300 in hCHIT1 (Ile300 in hAMCase) are conserved in both proteins, we believe that these
12 two compounds as well as compound **7f** bind in a similar way to the AMCase active site. However, the
13 increased potency seen against hAMCase compared to hCHIT1 could be explained by the fact that
14 residue 269 is an arginine in hCHIT1 whereas it is a histidine in the case of AMCase. In the case of
15 hCHIT1 the presence of a long positively charged side chain facing a hydrophobic function, either the
16 isopropyl or phenyl in compounds **7g** and **7i** respectively, may have a negative effect on compound
17 binding (distance with the phenyl group and Arg269 is 3.6 Å). In contrast, this is not the case with the
18 hAMCase as the N ϵ 2 and C ϵ 1 at the edge of the His269 imidazole ring establish van der Waals
19 contacts with the isopropyl group in compound **7g** and the phenyl group in compound **7i**. Taking all
20 these observations together and extrapolating them on hAMCase-inhibitor interaction, one can say that
21 the isopropyl group in compounds **7g** and **7f** as well as the phenyl group in compound **7i** enhance the
22 hydrophobic interaction with Ile300 and His269 in hAMCase leading to an improved stacking
23 conformation of Trp99 favoring the short H-bond between Glu140 and the water mediated compound
24 **7i** interaction. These contacts together with the strong bonds with Asp213, Tyr212, and Asp138
25 provide a mechanistic explanation of the higher selectivity of these inhibitors against hAMCase.
26 Further proof of this interpretation lays in the SAR analysis of compounds **7a-k**. An increase of the
27 size of R1 substituent along with augmenting its hydrophobic character led to the raise of both activity
28 and selectivity hAMCase vs. hCHIT1.
29
30
31
32
33
34
35
36
37
38
39
40
41
42
43
44
45
46
47
48
49
50
51

52 In parallel to optimization of the R1 substituent we have looked into modification of the
53 hydrophobic pocket binding fragment R2. The X-ray crystallographic data show that the benzyl group
54 in R2 establishes hydrophobic interaction with Tyr267, Glu297 and Met300 (Ile300 in hAMCase) side
55
56
57
58
59
60

chains allowing the accommodation of the R2 in this pocket (Fig 2D). The obtained structures reveal that the introduction of a halogen at the para position of the benzyl ring leads to an interaction between the C–X (X=Br or Cl) of the R2 function and the residue 295 side chain (Ala in hAMCase and Thr in hCHIT1) located at the bottom of the pocket. This interaction occurs within a distance of 3.5Å which increases the ligands potency toward the human chitinases. Removing the halogen group or substituting it with a bigger hydrophobic function as in compounds **7m** to **7r** (see Table 2) highly decreased the compounds activity. This diminution is most likely due to the steric hindrance caused by these functions which would create clashes with residue 295 side chains perturbing the accommodation of R2 function in this hydrophobic pocket. Thus, the optimal function selected for R2 is the para-halogenated phenethyl. Any deviation from p-Br-phenethyl or p-Cl-phenethyl substituents led to decreased activity, with the small alkyl para-substituted phenethyl fragment being the closest in activity and para-cyclopropyl i.e. inhibitor **7p** the best. Compounds **7l-s** are samples of variations we have tried.²³

Along with the optimization of the in vitro potency and selectivity, some of the representative inhibitors were evaluated for their in vitro ADME and in vivo pharmacokinetic properties.

Table 3. In Vivo Pharmacokinetic Profile of Selected Analogues after iv Dose at 3 mg/kg in Mice

Compound	V _{ss} (L/kg)	CL (mL/min/kg)	T _{1/2} (h)	AUC _{0-inf} (mg*h/L)
7a	12.8	52.6	4.40	0.95
7f	2.33	9.06	2.97	5.52
7g	1.66	8.53	3.25	5.86
7j	3.03	45.0	6.78	1.11
15a	1.16	11.5	11.1	4.34

Table 4. In Vivo Pharmacokinetic Profile of Selected Analogues after Oral Dose at 10 mg/kg in Mice and Microsomal Stability (% remaining after 20 min).

Compound	C _{max} (mg/L)	T _{max} (h)	AUC _{0-inf} (mg*h/L)	F (%)	LM Stb
7a	0.672	2.0	3.34	99	97.5

7f	1.86	0.25	9.56	52	76.9
7g	6.04	0.5	27.9	100	78.3
7j	0.618	1.0	1.75	47	21
15a	3.25	1.0	8.21	57	100

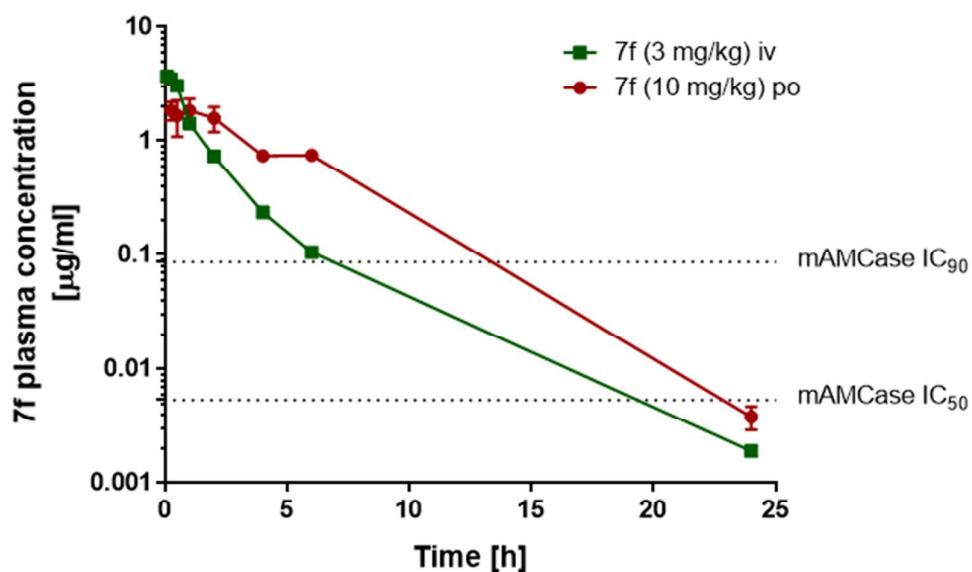


Figure 4. Plasma concentration–time course for compound **7f** after 3 mg/kg iv bolus and after 10 mg/kg oral administration (po) into female BALB/c mice.

Microsomal stability showed, in general, a good correlation to in vivo clearance and po exposure in mice, indicating hepatic first pass is the likely driver of oral bioavailability and phase I metabolism is the major clearance route for this series. Overall, compounds **7f**, **7g** and **15a** showed good oral bioavailability, low to moderate clearance, and adequate exposure for efficacy testing following once daily po dosing in mice. Compounds **7a** and **7j** had higher clearances and lower systemic absorption and may require twice daily po dosing. Inhibitor **7f** was chosen to be tested in animal models of asthma.

A common and clinically relevant aeroallergen HDM extract was used to induce acute allergic airway inflammation in BALB/c mice. HDM administration for three consecutive weeks resulted in increased leukocytes influx to the lungs (particularly eosinophils) and increased IgE concentration in the plasma of mice challenged with HDM as compared to control group. These changes were accompanied by a

significant increase in the chitinolytic activity in bronchoalveolar lavage fluid (BALF) (Fig. 5). Oral treatment with the compound **7f** (30 mg/kg), in a therapeutic scheme starting from day 7 after the start of HDM administration led to a significant reduction in total leukocyte numbers (Fig. 5A), particularly the eosinophil numbers (Fig. 5B) in BALF as compared to vehicle-treated controls. Significant anti-inflammatory effects of compound **7f** corresponded with reduced chitinase activity in BALF (Fig. 5C), as well as a significant reduction of total plasma IgE concentration (Fig. 5D).

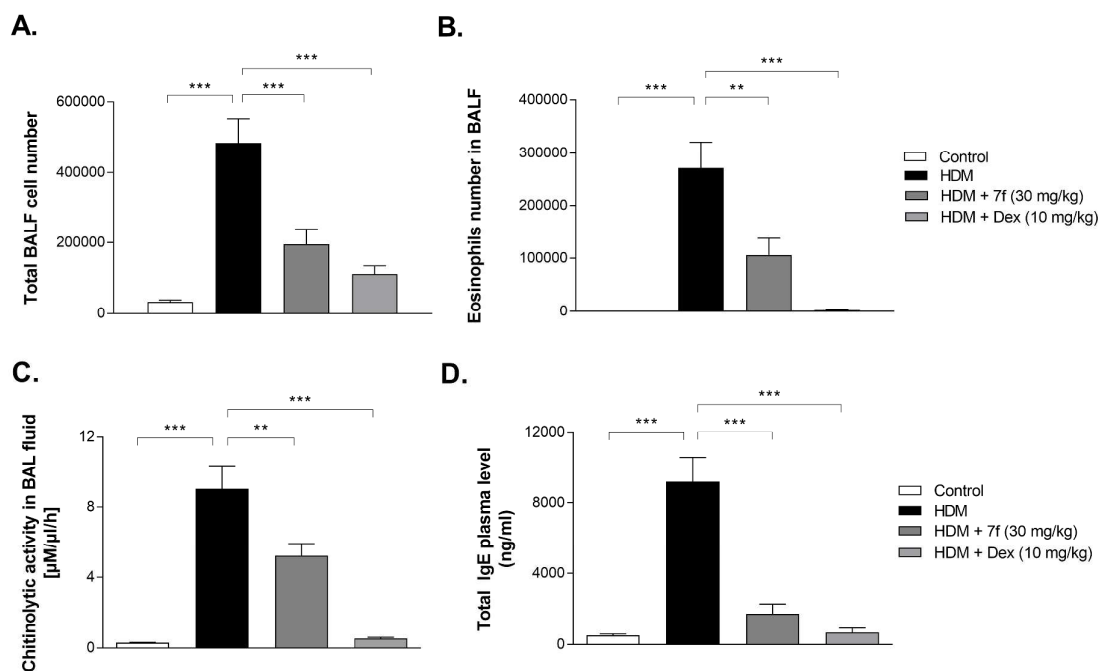
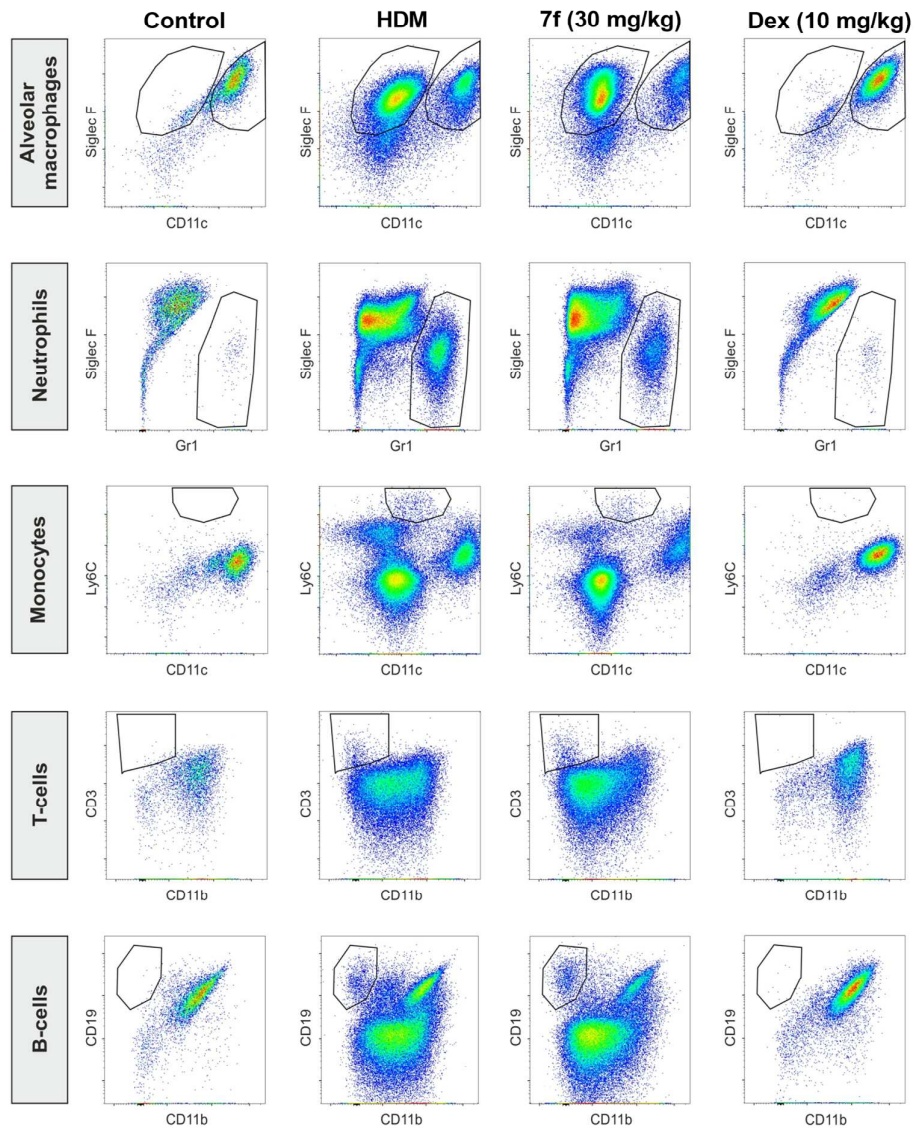


Figure 5. Selective AMCcase inhibition with compound **7f** exerts significant anti-inflammatory effects in HDM-induced asthma model in mice. Dexamethasone (Dex) was administered ip and **7f** was given po starting from day 7 after the start of HDM administration. (A) Total leukocyte numbers in BAL (n = 8). (B) Flow cytometry analysis of eosinophils (Siglec F+, CD11c-) represented as total eosinophil numbers in BAL isolated from mice challenged with PBS (Control) or HDM for 3 consecutive weeks with or without **7f** or dexamethasone treatment. (C) Chitinolytic activity in BAL. (D) Total IgE level in plasma. Data are mean \pm s.e.m. $**P < 0.01$; $***P < 0.001$; by one-way ANOVA followed by Tukey's multiple-comparison test.

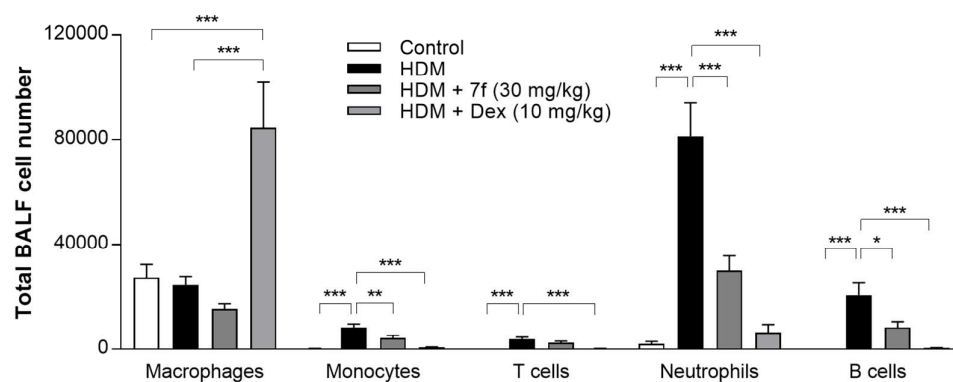
In addition, flow cytometry analysis of BAL leukocyte subpopulations revealed that compound **7f** treatment significantly reduced the total numbers of other subtypes of infiltrating (CD45+) leukocytes

1
2
3 such as neutrophils, monocytes and B cells in BALF (Fig. 6). T cells (CD3+) show only trend towards
4 reduction in numbers after **7f** treatment without statistical significance. Anti-inflammatory efficacy of
5 compound **7f** was observed in three independent acute HDM-induced asthma experimental conditions.
6
7
8
9
10
11
12
13
14
15
16
17
18
19
20
21
22
23
24
25
26
27
28
29
30
31
32
33
34
35
36
37
38
39
40
41
42
43
44
45
46
47
48
49
50
51
52
53
54
55
56
57
58
59
60

A.



B.



1
2
3 **Figure 6.** Selective AMCase inhibition with compound **7f** decreases the numbers of different
4 leukocyte subpopulations in BAL in HDM-induced allergic airway inflammation in mice.
5 Dexamethasone (Dex) was administered ip and **7f** was given po starting from day 7 after the start of
6 HDM administration. (A) Representative flow cytometry analysis of leukocyte subpopulations such as
7 alveolar macrophages, eosinophils, neutrophils, monocytes, T and B cells gated from the CD45⁺
8 BALF leukocytes isolated from mice challenged with PBS or HDM for 3 consecutive weeks with or
9 without **7f** or dexamethasone treatment. (B) Quantitative flow cytometry analysis of leukocyte
10 numbers such as alveolar macrophages, neutrophils, monocytes, T and B cells in BAL. Data are mean
11 \pm s.e.m. * $P < 0.01$; ** $P < 0.01$; *** $P < 0.001$; by one-way ANOVA followed by Tukey's multiple-
12 comparison test.
13
14
15
16
17
18
19
20
21
22
23

24 Considering the overall activity profile of compound **7f**, it was further characterized. To fully
25 determine its affinity towards h/mAMCase and h/mCHIT1, inhibitory constants (K_i) for all four
26 enzymes have been measured and they are in good correlation with earlier established IC_{50} data
27 (hAMCase $K_i = 13.5 \pm 2.4$; hCHIT1 $K_i = 312 \pm 205$; mAMCase $K_i = 10.5 \pm 1.6$; mCHIT1 $K_i = 3404$
28 ± 1749 nM). Compound **7f** has passed the test for genotoxicity (AMES test²⁴ was negative) but
29 showed a potential for cardiotoxicity (hERG binding²⁵ activity IC_{50} 4 μ M). Off-target in vitro effects
30 of compound **7f** have been evaluated in the CEREP DiversityTM panel consisting of 72 binding and 27
31 enzyme assays²⁶ and revealed interactions with mono-amine transporters for serotonin and dopamine
32 (95% inhibition at 10 μ M for both).
33
34
35
36
37
38
39
40
41
42
43

44 CONCLUSIONS:

45
46 A new series of aminotriazoles with a high inhibitory activity against human and mouse
47 chitinases (AMCase and CHIT1) has been identified. Structural biology analysis guided medicinal
48 chemistry efforts, leading to the discovery of several highly potent and selective (AMCase vs CHIT1)
49 inhibitors. Pharmacokinetic profiles of the top five compounds were further analyzed, resulting in the
50 nomination of inhibitor **7f** for pre-development level screening.
51
52
53
54
55
56
57
58
59
60

1
2
3 Overall compound **7f** is a highly potent, selective (the mouse enzyme) AMCcase inhibitor with
4 very good PK properties. Once daily 30 mg/kg oral doses in mice showed significant anti-
5 inflammatory efficacy in acute HDM-induced allergic airway inflammation mainly by providing
6 significant reduction in total IgE levels in plasma, correlating with reduction of AMCcase activity and
7 inflammatory cell influx in the BALF as compared to vehicle controls. Therapeutic efficacy of
8 compound **7f** in the clinically relevant aeroallergen-induced acute asthma model in mice suggests
9 significant therapeutic potential to treat asthma patients alone or in a combination with first line
10 existing therapies. Further development of compound **7f** was not pursued because of the concerns of
11 potential cardiovascular safety margin versus hERG and its activity against the dopamine transporter,
12 but this orally active and highly selective AMCcase inhibitor can serve as valuable tool in future studies
13 on the role of AMCcase in various pathologies.
14
15
16
17
18
19
20
21
22
23

24 Samples of compounds **7f** will be provided, when possible, to facilitate further preclinical
25 research on the role of AMCcase in asthma and other relevant diseases. Please contact the
26 corresponding author for details.
27
28
29
30
31

32 **EXPERIMENTAL SECTION:**

33
34 **Chemical Methods.** All solvents, substrates and reagents that were commercially available were used
35 without further purification. TLC analysis was performed using pre-coated glass plates (0.2 ± 0.03 mm
36 thickness, GF-254, particle size 0.01–0.04 mm) from Fluorochem Ltd, UK. Column chromatography
37 was performed using high-purity grade silica gel (pore size 60 Å, 220-440 mesh particle size, 35-75
38 µm particle size) from Fluka. Preparative HPLC was performed on LC-20AP Shimadzu with ELSD-
39 LTII detector equipped with Hypersil GOLD 21.2/250 mm, 5 µm C18 column. ¹H NMR spectra were
40 recorded on Bruker AVANCE II PLUS NMR spectrometers at 700 MHz. All spectra were recorded in
41 appropriate deuterated solvents (CDCl₃, DMSO-d₆, D₂O, CD₃OD, etc.) that were commercially
42 available. Resonances are given in parts per million relative to tetramethylsilane. Data are reported as
43 follows: chemical shift, multiplicity (s = singlet, d = doublet, t = triplet, m = multiplet, bs = broad
44 singlet, bd = broad doublet), coupling constants (J in Hz) and integration. ESI-MS spectra were
45 recorded on a Shimadzu LC-20AD LPG separation module with a SPD-M20A UV detector and
46
47
48
49
50
51
52
53
54
55
56
57
58
59
60

1
2
3 LCMS-2020 mass detector equipped with Kinetex 2.1/50 mm, 2.6 μ m C18 column eluted with 0.5
4 mL/min flow of 10-90% gradient (over 6 min) of acetonitrile in water. HRMS-ESI spectra were
5 recorded on Bruker Maxis Impact instrument. Purities of all reported compounds were greater than
6 95% based on elemental analysis and/or HPLC chromatograms. HPLC analyses were performed on a
7 Waters Acquity UPLC system fitted with BEH C18 1.7 μ m column (2.1 \times 50 mm) and with UV
8 detection (220 nm), gradient 3-97% of acetonitrile in water, flow 0.6mL/min over 3min.
9
10
11
12
13
14
15

16 **1-(4-(3-Amino-1H-1,2,4-triazol-5-yl)piperazin-1-yl)-2-(4-bromophenoxy)ethanone hydrochloride**
17
18 (4).
19

20 Step 1: Synthesis of *tert-butyl 4-(2-(4-bromophenoxy)acetyl)piperazine-1-carboxylate (3)*. 4-
21 Bromophenoxyacetic acid **2** (250 mg, 1.08 mmol) was dissolved in dichloromethane (5 mL),
22 diisopropylethylamine (0.23 mL, 1.29 mmol) was added at ambient temperature followed by addition
23 of Boc-piperazine (201 mg, 1.08 mmol), and when the solution was clear the coupling reagent TBTU
24 (347 mg, 1.29 mmol) was added. The reaction mixture was stirred at ambient temperature overnight,
25 diluted with dichloromethane and washed with 1 M aq NaOH, 2 M aq HCl, brine and dried over
26 MgSO₄. The solvent was evaporated and the product was purified by flash chromatography (gradient
27 elution 0-1% methanol in dichloromethane) to afford pure amide **3** as off-white foam (380 mg, 88%).
28 LC-MS (ES⁺): RT 5.5 min, m/z 399.1/401.1 [M+H]⁺. ¹H NMR (700 MHz, CDCl₃) δ 7.41 (d, *J* = 9.1
29 Hz, 2H), 6.86 (d, *J* = 9.1 Hz, 2H), 4.70 (s, 2H), 3.62 – 3.53 (m, 4H), 3.46 – 3.30 (m, 4H), 1.49 (s, 9H).
30
31
32
33
34
35
36
37
38
39

40 Step 2: Synthesis of *1-(4-(3-amino-1H-1,2,4-triazol-5-yl)piperazin-1-yl)-2-(4-bromophenoxy)ethanone*
41 *hydrochloride (4)*. The N-Boc protected amine **3** (350 mg, 0.87 mmol) was dissolved in ethyl acetate
42 (2 mL) and treated with a hydrogen chloride (4 M solution in ethyl acetate, 5 mL). The reaction
43 mixture was stirred at ambient temperature and controlled by TLC (chloroform/methanol 9:1). When
44 substrate was no longer detected the precipitate was filtered and washed with ether to give amine as
45 hydrochloride salt (280 mg, 95%), which was sufficiently pure to be used in the following step. The
46 hydrochloride salt of the amine (137 mg, 0.41 mmol), anhydrous potassium carbonate (143 mg, 1.03
47 mmol) and S,S'-dimethyl-N-cyano-dithioiminocarbonate (61 mg, 0.41 mmol) were added to
48 acetonitrile (4 mL) and the reaction mixture was refluxed for 3 h (monitoring by TLC). Hydrazine
49
50
51
52
53
54
55
56
57
58
59
60

1
2
3 monohydrate (0.06 mL, 1.24 mmol) was then added and the mixture was further refluxed for another 2
4 h. After this time it was cooled to room temperature and solids were filtered off. The filtrate was
5 concentrated in vacuo and the crude product was purified by flash chromatography (gradient elution 1-
6 5% methanol in dichloromethane), then was converted into hydrochloride salt by hydrogen chloride
7 (4M solution in ethyl acetate), washed with ether and dried in vacuo to give title compound **4** as white
8 solid (71 mg, 62%), mp 193-194°C. LC-MS (ES+): RT 3.8 min, m/z 381.0/383.0 [M+H]⁺. ¹H NMR
9 (700 MHz, DMSO-d₆) δ 7.39 (d, *J* = 9.0 Hz, 2H), 6.88 (d, *J* = 9.0 Hz, 2H), 4.79 (s, 2H), 3.62 – 3.49
10 (m, 4H), 3.29 (bs, 4H). HRMS calculated for C₁₄H₁₈BrN₆O₂ [M+H]⁺ 381.0669, found 381.0663.
11
12
13
14
15
16
17
18
19

20
21 **General Procedure for the Synthesis of 1-(3-Amino-1H-1,2,4-triazol-5-yl)-N-(R2)-substituted-N-**
22 **(4-(R1)-substituted-phenethyl)piperidin-4-amine (7a-7s).**
23

24 **1-(3-Amino-1H-1,2,4-triazol-5-yl)-N-(4-bromophenethyl)-N-methylpiperidin-4-amine (7a).**
25

26 Step 1: Synthesis of *tert-butyl 4-((4-chlorophenethyl)(methyl)amino)piperidine-1-carboxylate (6a)*. To
27 a stirred solution of N-Boc-4-piperidone (200 mg, 1 mmol) and 4-bromophenethylamine (0.18 mL, 1.2
28 mmol) in 1,2-dichloroethane (3 mL), sodium triacetoxyborohydride (424 mg, 2 mmol) was added. The
29 reaction mixture was stirred at ambient temperature overnight. Then, 30% aqueous formaldehyde
30 solution (0.45 mL, 5 mmol) and second portion of sodium triacetoxyborohydride (424 mg, 2 mmol)
31 were added. The stirring was continued for 1 h. A 5% solution of sodium bicarbonate was added (6
32 mL) and the biphasic mixture was stirred for 30 minutes. The layers were separated and the aqueous
33 layer was additionally extracted with dichloromethane (2 × 5 mL). The combined organic extracts
34 were then dried over MgSO₄, and solvent was removed in vacuo. The crude residue was purified by
35 flash chromatography (gradient elution 1-1.5% methanol in dichloromethane) to afford title compound
36 **6a** as colorless oil (300 mg, 75%). LC-MS (ES+): RT 4.3 min, m/z 397.0/399.0 [M+H]⁺. ¹H NMR
37 (700 MHz, CDCl₃) δ 7.39 (d, *J* = 8.3 Hz, 2H), 7.07 (d, *J* = 8.3 Hz, 2H), 4.17 – 4.11 (m, 2H), 2.72 –
38 2.67 (m, 6H), 2.57 – 2.52 (m, 1H), 2.34 (s, 3H), 1.74 – 1.71 (m, 2H), 1.45 (s, 9H), 1.43 – 1.37 (m, 2H).
39
40
41
42
43
44
45

46 Step 2: Synthesis of *1-(3-Amino-1H-1,2,4-triazol-5-yl)-N-(4-bromophenethyl)-N-methylpiperidin-4-*
47 *amine (7a)*. The N-Boc protected amine **3** (300 mg, 0.75 mmol) was dissolved in ethyl acetate (2 mL)
48 and treated with a hydrogen chloride (4 M solution in ethyl acetate, 5 mL). The reaction mixture was
49
50
51
52
53
54
55
56
57
58
59
60

1
2
3 stirred at ambient temperature and controlled by TLC (chloroform/methanol 9:1). When substrate was
4 no longer detected the precipitate was filtered and washed with ether to give amine as hydrochloride
5 salt (270 mg, 97%), which was sufficiently pure to be used in the following step. The hydrochloride
6 salt of the amine (270 mg, 0.73 mmol), anhydrous potassium carbonate (251 mg, 1.82 mmol) and
7 S,S'-dimethyl-N-cyano-dithioiminocarbonate (107 mg, 0.73 mmol) were added to acetonitrile (4 mL)
8 and the reaction mixture was refluxed for 3 h (monitoring by TLC). Hydrazine monohydrate (0.11 mL,
9 2.19 mmol) was then added and the mixture was further refluxed for another 2 h. After this time it was
10 cooled to room temperature and solids were filtered off. The filtrate was concentrated in vacuo and the
11 crude product was purified by flash chromatography (gradient elution 1-5% methanol in
12 dichloromethane), then was crystallized from acetonitrile to give title compound **7a** (170 mg, 62%),
13 mp 152-153°C. LC-MS (ES+): RT 1.0 min, m/z 379.2/ 381.2 [M+H]⁺. ¹H NMR (700 MHz, DMSO-d₆
14 + D₂O) δ 7.40 (d, *J* = 8.3 Hz, 2H), 7.15 (d, *J* = 8.3 Hz, 2H), 3.73 (d, *J* = 12.9 Hz, 2H), 2.62 (dd, *J* =
15 9.2, 5.9 Hz, 2H), 2.61 – 2.54 (m, 4H), 2.48 – 2.40 (m, 1H), 2.17 (s, 3H), 1.62 (d, *J* = 14.9 Hz, 2H),
16 1.31 (qd, *J* = 12.4, 4.1 Hz, 2H). Elemental analysis calculated (%) for C₁₆H₂₃BrN₆: C 50.67, H 6.11, N
17 22.16. Found: C 50.56, H 6.04, N 22.08.

18
19
20
21
22
23
24
25
26
27
28
29
30
31
32
33 **1-(3-Amino-1H-1,2,4-triazol-5-yl)-N-(4-chlorophenethyl)-N-methylpiperidin-4-amine**

34 **trihydrochloride (7b)**. The title compound was prepared by a similar procedure as that used for **7a**
35 and purified by preparative HPLC to give **7b** as hydrochloride salt (40 mg, 76%), mp 162-164°C. LC-
36 MS (ES+): RT 0.9 min, m/z 335.1/ 337.1 [M+H]⁺. ¹H NMR (700 MHz, DMSO-d₆ + D₂O) δ 7.37 –
37 7.34 (m, 2H), 7.33 – 7.30 (m, 2H), 3.82 (d, *J* = 13.0 Hz, 2H), 3.50 (tt, *J* = 12.2, 3.6 Hz, 1H), 3.36 –
38 3.27 (m, 1H), 3.24 – 3.15 (m, 1H), 3.07 – 2.89 (m, 4H), 2.75 (s, 3H), 2.12 – 1.91 (m, 2H), 1.77 – 1.59
39 (m, 2H). HRMS calculated for C₁₆H₂₄ClN₆ [M+H]⁺ 335.1745, found 335.1736.

40
41
42
43
44
45
46 **1-(3-Amino-1H-1,2,4-triazol-5-yl)-N-(4-chlorophenethyl)-N-ethylpiperidin-4-amine (7c)**. The title
47 compound was prepared by a similar procedure as that used for **7a** and crystallized from acetonitrile to
48 give **7c** (296 mg, 62%), mp 141-142°C. LC-MS (ES+): RT 1.1min, m/z 349.3/ 351.3 [M+H]⁺. ¹H
49 NMR (700 MHz, DMSO-d₆ + D₂O) δ 7.28 – 7.24 (m, 2H), 7.22 – 7.17 (m, 2H), 3.77-3.74 (m, 2H),
50 2.62 – 2.58 (m, 3H), 2.58-2.54 (m, 3H), 1.60 (d, *J* = 11.4 Hz, 2H), 1.31 (qd, *J* = 12.3, 4.0 Hz, 2H),
51
52
53
54
55
56
57
58
59
60

0.90 (t, $J = 7.1$ Hz, 3H), three protons overlapping with water and DMSO signals. Elemental analysis calculated (%) for $C_{17}H_{25}ClN_6$: C 58.53, H 7.22, N 24.09. Found: C 58.66, H 7.32, N 24.10.

1-(3-Amino-1H-1,2,4-triazol-5-yl)-N-(4-bromophenethyl)-N-ethylpiperidin-4-amine (7d). The title compound was prepared by a similar procedure as that used for **7a** and crystallized from acetonitrile to give **7d** (150 mg, 52%), mp 137-138°C. LC-MS (ES+): RT 1.7 min, m/z 393.2/ 395.2 $[M+H]^+$. 1H NMR (700 MHz, DMSO- d_6 + D_2O) δ 7.39 – 7.36 (m, 2H), 7.15 – 7.11 (m, 2H), 3.77 – 3.74 (m, 2H), 2.63 – 2.59 (m, 7H), 2.51 (q, $J = 7.1$ Hz, 2H), 1.60 (d, $J = 10.5$ Hz, 2H), 1.34 (qd, $J = 12.3, 4.3$ Hz, 2H), 0.91 (t, $J = 7.1$ Hz, 3H). Elemental analysis calculated (%) for $C_{17}H_{25}BrN_6$: C 51.91, H 6.41, N 21.37. Found: C 51.89, H 3.37, N 21.33.

1-(3-Amino-1H-1,2,4-triazol-5-yl)-N-(4-chlorophenethyl)-N-isopropylpiperidin-4-amine trihydrochloride (7e). The title compound was prepared by a similar procedure as that used for **7a** and purified by preparative HPLC to give **7e** as hydrochloride salt (50 mg, 44%), mp 88-89°C. LC-MS (ES+): RT 2.0 min, m/z 363.0/ 365.0 $[M+H]^+$. 1H NMR (700 MHz, DMSO- d_6 + D_2O) δ 7.38 – 7.35 (m, 2H), 7.35 – 7.32 (m, 2H), 3.85 – 3.79 (m, 3H), 3.55 (tt, $J = 11.9, 3.4$ Hz, 1H), 3.30 – 3.18 (m, 2H), 3.02 – 2.91 (m, 4H), 2.13 – 2.04 (m, 2H), 1.85 – 1.72 (m, 2H), 1.32 (d, $J = 6.5$ Hz, 3H), 1.24 (d, $J = 6.5$ Hz, 3H). Elemental analysis calculated (%) for $C_{18}H_{27}ClN_6 \cdot 3HCl \cdot H_2O$: C 44.10, H 6.58, N 17.14. Found: C 44.18, H 6.91, N 16.76.

1-(3-Amino-1H-1,2,4-triazol-5-yl)-N-(4-chlorophenethyl)-N-isobutylpiperidin-4-amine (7f). The title compound was prepared by a similar procedure as that used for **7a** and purified by crystallization from acetonitrile to give **7f** (220 mg, 42%), mp 127-128°C. LC-MS (ES+): RT 3.1 min, m/z 377.3/ 379.3 $[M+H]^+$. 1H NMR (700 MHz, DMSO- d_6 + D_2O) δ 7.25 (d, $J = 8.0$ Hz, 2H), 7.18 (d, $J = 8.0$ Hz, 2H), 3.77 – 3.64 (m, 2H, overlapping with water), 2.64 – 2.53 (m, 7H), 2.09 (d, $J = 7.1$ Hz, 2H), 1.61 – 1.40 (m, 3H), 1.32 – 1.24 (m, 2H), 0.71 (d, $J = 6.5$ Hz, 6H). Elemental analysis calculated (%) for $C_{19}H_{29}ClN_6$: C 60.54, H 7.76, N 22.30. Found: C 60.61, H 7.72, N 22.17.

1-(3-Amino-1H-1,2,4-triazol-5-yl)-N-(4-bromophenethyl)-N-isobutylpiperidin-4-amine (7g). The title compound was prepared by a similar procedure as that used for **7a** and purified by crystallization from acetonitrile to give **7g** (305 mg, 62%), mp 127-128°C. LC-MS (ES+): RT 3.4 min, m/z 421.25/ 423.25 $[M+H]^+$. 1H NMR (700 MHz, DMSO- d_6 + D_2O) δ 7.38 (d, $J = 8.2$ Hz, 2H), 7.12 (d, $J = 8.2$ Hz,

2H), 3.77 – 3.71 (m, 2H, overlapping with water), 2.60 – 2.51 (m, 7H), 2.09 (d, $J = 6.6$ Hz, 2H), 1.56 – 1.49 (m, 2H), 1.46 – 1.43 (m, 1H), 1.33 – 1.24 (m, 2H), 0.71 (d, $J = 6.4$ Hz, 6H). Elemental analysis calculated (%) for $C_{19}H_{29}BrN_6$: C 54.16, H 6.94, N 19.94. Found: C 54.20, H 6.84, N 19.95.

1-(3-Amino-1H-1,2,4-triazol-5-yl)-N-(4-chlorophenethyl)-N-(cyclohexylmethyl)piperidin-4-amine trihydrochloride (7h). The title compound was prepared by a similar procedure as that used for **7a** and purified by preparative HPLC to give **7h** as hydrochloride salt (32 mg, 53%), mp 154-155°C. LC-MS (ES+): RT 3.9 min, m/z 417.5/419.5 $[M+H]^+$. 1H NMR (700 MHz, DMSO- d_6 + D_2O) δ 7.37 (d, $J = 8.4$ Hz, 2H), 7.33 (d, $J = 8.4$ Hz, 2H), 3.83 (bd, $J = 12.9$ Hz, 2H), 3.56 – 3.52 (m, 1H), 3.29 – 3.20 (m, 2H), 3.07 (dd, $J = 13.7, 7.7$ Hz, 1H), 3.00 (t, $J = 8.5$ Hz, 2H), 2.96 – 2.89 (m, 3H), 2.04 (bd, $J = 10.3$ Hz, 1H), 1.97 (bd, $J = 12.1$ Hz, 1H), 1.81 (bd, $J = 11.6$ Hz, 1H), 1.75 – 1.64 (m, 6H), 1.61 – 1.58 (m, 1H), 1.25 – 1.18 (m, 2H), 1.11 (tt, $J = 12.8, 3.2$ Hz, 1H), 0.99 – 0.91 (m, 2H). Elemental analysis calculated (%) for $C_{22}H_{33}ClN_6 \cdot 3HCl \cdot H_2O$: C 48.54, H 7.04, N 15.44. Found: C 48.74, H 6.79, N 15.81.

1-(3-Amino-1H-1,2,4-triazol-5-yl)-N-benzyl-N-(4-chlorophenethyl)piperidin-4-amine (7i). The title compound was prepared by a similar procedure as that used for **7a** and purified by crystallization from acetonitrile to give **7i** (77 mg, 51%), mp 51-52°C. LC-MS (ES+): RT 3.6 min, m/z 411.3/413.3 $[M+H]^+$. 1H NMR (700 MHz, DMSO- d_6 + D_2O) δ 7.25 – 7.18 (m, 6H), 7.18 – 7.13 (m, 1H), 7.08 (d, $J = 8.0$ Hz, 2H), 3.78- 3.68 (m, 2H), 3.60 (bs, 2H), 2.66 – 2.52 (m, 6H), 1.62 (bd, $J = 12.2$ Hz, 2H), 1.38 (qd, $J = 12.0, 3.9$ Hz, 2H), one proton overlapping with DMSO signals. HRMS calculated for $C_{22}H_{28}ClN_6$ $[M+H]^+$ 411.2058, found 411.2064.

1-(3-Amino-1H-1,2,4-triazol-5-yl)-N-(2-chlorobenzyl)-N-(4-chlorophenethyl)piperidin-4-amine (7j). The title compound was prepared by a similar procedure as that used for **7a** and purified by crystallization from acetonitrile to give **7j** (28 mg, 64%), mp 88-89°C. LC-MS (ES+): RT 3.7 min, m/z 445.3/447.3 $[M+H]^+$. 1H NMR (700 MHz, DMSO- d_6 + D_2O) δ 7.35 – 7.33 (m, 1H), 7.33 – 7.30 (m, 1H), 7.22 (d, $J = 8.3$ Hz, 2H), 7.20 – 7.17 (m, 2H), 7.09 (d, $J = 8.3$ Hz, 2H), 3.81-3.79 (m, 2H), 3.76-3.74 (m, 1H), 3.68 (s, 2H), 2.68 – 2.62 (m, 3H), 2.57 (t, $J = 7.2$ Hz, 3H), 1.63 (d, $J = 12.0$ Hz, 2H), 1.38 (qd, $J = 13.4, 4.6$ Hz, 2H). Elemental analysis calculated (%) for $C_{22}H_{26}Cl_2N_6$: C 59.33, H 5.88, N 18.87. Found: C 59.35, H 5.85, N 18.67.

1
2
3 **1-(3-Amino-1H-1,2,4-triazol-5-yl)-N-(4-chlorophenethyl)-N-(naphthalen-1-ylmethyl)piperidin-4-**
4 **amine trihydrochloride (7k).** The title compound was prepared by a similar procedure as that used
5 for **7a** and purified by preparative HPLC to give **7k** as hydrochloride salt (140 mg, 64%), mp 145-
6 146°C. LC-MS (ES+): RT 4.1 min, m/z 461.4/463.4 [M+H]⁺. ¹H NMR (700 MHz, DMSO-d₆ + D₂O) δ
7 8.18 (d, *J* = 9.0 Hz, 1H), 8.04 (d, *J* = 8.3 Hz, 1H), 8.01 (d, *J* = 8.0 Hz, 1H), 7.81 (d, *J* = 7.1 Hz, 1H),
8 7.67 – 7.65 (m, 1H), 7.62 – 7.57 (m, 2H), 7.24 (d, *J* = 8.5 Hz, 2H), 6.99 (d, *J* = 8.5 Hz, 2H), 4.84 (bs,
9 2H), 3.92 (bd, *J* = 13.4 Hz, 2H), 3.67 – 3.63 (m, 1H), 3.27 – 3.24 (m, 2H), 2.97 – 2.93 (m, 2H), 2.82 –
10 2.78 (m, 2H), 2.22 (d, *J* = 12.4 Hz, 2H), 1.97 (qd, *J* = 12.1, 4.2 Hz, 2H). Elemental analysis calculated
11 (%) for C₂₆H₂₉ClN₆*3HCl*H₂O: C 54.75, H 5.66, N 14.73. Found: C 54.82, H 5.48, N 14.90.

12
13
14
15
16
17
18
19
20 **1-(3-Amino-1H-1,2,4-triazol-5-yl)-N-methyl-N-phenethylpiperidin-4-amine trihydrochloride (7l).**
21 The title compound was prepared by a similar procedure as that used for **7a** and purified by
22 preparative HPLC to give **7l** as hydrochloride salt (33 mg, 38%), mp 158-160°C. LC-MS (ES+): RT
23 0.4 min, m/z 301.2 4 [M+H]⁺. ¹H NMR (700 MHz, DMSO-d₆ + D₂O) δ 7.34 – 7.29 (m, 4H), 7.25 (t, *J*
24 = 7.1 Hz, 1H), 3.84 (bd, *J* = 12.6 Hz, 2H), 3.54 – 3.49 (m, 1H), 3.37 – 3.33 (m, 1H), 3.25 – 3.21 (m,
25 1H), 3.06 – 3.01 (m, 1H), 2.99 – 2.92 (m, 3H), 2.77 (s, 3H), 2.04 – 2.01 (m, 2H), 1.75 – 1.64 (m, 2H).
26 Elemental analysis calculated (%) for C₁₆H₂₄N₆*3HCl: C 46.90, H 6.64, N 20.51. Found: C 46.61, H
27 6.86, N 20.37.

28
29
30
31
32
33
34
35
36 **1-(3-Amino-1H-1,2,4-triazol-5-yl)-N-methyl-N-(4-methylphenethyl)piperidin-4-amine (7m).** The
37 title compound was prepared by a similar procedure as that used for **7a** and crystallized from
38 acetonitrile to give **7m** (27 mg, 37%), mp 150-152°C. LC-MS (ES+): RT 0.7 min, m/z 315.2 [M+H]⁺.
39 ¹H NMR (700 MHz, DMSO-d₆ + D₂O) δ 7.19 (d, *J* = 8.0 Hz, 2H), 7.14 (d, *J* = 8.0 Hz, 2H), 3.85 (d, *J*
40 = 13.6 Hz, 2H), 3.52 (tt, *J* = 11.8, 3.4 Hz, 1H), 3.33 (td, *J* = 11.6, 5.2 Hz, 1H), 3.20 (td, *J* = 11.9, 5.5
41 Hz, 1H), 3.02 – 2.89 (m, 4H), 2.78 (s, 3H), 2.26 (s, 3H), 2.07 – 2.00 (m, 2H), 1.77 – 1.64 (m, 2H).
42 HRMS calculated for C₁₇H₂₇N₆ [M+H]⁺ 315.2292, found 315.2289.

43
44
45
46
47
48
49
50 **1-(3-Amino-1H-1,2,4-triazol-5-yl)-N-(4-ethylphenethyl)-N-methylpiperidin-4-amine**
51 **dihydrochloride (7n).** The title compound was prepared by a similar procedure as that used for **7a**
52 and purified by preparative HPLC to give **7n** as hydrochloride salt (88 mg, 45%), mp 163-164°C. LC-
53 MS (ES+): RT 1.7 min, m/z 329.4 [M+H]⁺. ¹H NMR (700 MHz, DMSO-d₆ + D₂O) δ 7.22 (d, *J* = 8.1

1
2
3 Hz, 2H), 7.17 (d, $J = 8.1$ Hz, 2H), 3.85 (bd, $J = 13.0$ Hz, 2H), 3.53 – 3.49 (m, 1H), 3.36 – 3.31 (m,
4
5 1H), 3.23 – 3.19 (m, 1H), 3.02 – 2.98 (m, 1H), 2.96 – 2.90 (m, 3H), 2.78 (s, 3H), 2.56 (q, $J = 7.6$ Hz,
6
7 2H), 2.02 (bd, $J = 12.4$ Hz, 2H), 1.74 – 1.64 (m, 2H), 1.14 (t, $J = 7.6$ Hz, 3H). Elemental analysis
8
9 calculated (%) for $C_{18}H_{28}N_6 \cdot 2HCl \cdot 0.5H_2O$: C 52.68, H 7.61, N 20.48. Found: C 52.63, H 7.22, N
10
11 20.11.

12
13 **1-(3-Amino-1H-1,2,4-triazol-5-yl)-N-(4-isopropylphenethyl)-N-methylpiperidin-4-amine**

14
15 **trihydrochloride (7o)**. The title compound was prepared by a similar procedure as that used for **7a**
16
17 and purified by preparative HPLC to give **7o** as hydrochloride salt (147 mg, 52%), mp 157-158°C.
18
19 LC-MS (ES+): RT 3.3 min, m/z 343.1 $[M+H]^+$. 1H NMR (700 MHz, DMSO- d_6 + D_2O) δ 7.20 (d, $J =$
20
21 8.2 Hz, 2H), 7.17 (d, $J = 8.2$ Hz, 2H), 3.82 (d, $J = 12.9$ Hz, 2H), 3.50 (tt, $J = 11.9, 3.3$ Hz, 1H), 3.30
22
23 (td, $J = 12.3, 5.3$ Hz, 1H), 3.18 (td, $J = 12.2, 5.2$ Hz, 1H), 3.02 – 2.87 (m, 4H), 2.82 (sept, $J = 6.9$ Hz,
24
25 1H), 2.75 (s, 3H), 2.06 – 1.97 (m, 2H), 1.75 – 1.63 (m, 2H), 1.14 (d, $J = 6.9$ Hz, 6H). Elemental
26
27 analysis calculated (%) for $C_{19}H_{30}N_6 \cdot 3HCl$: C 50.50, H 7.36, N 18.60. Found: C 50.19, H 7.76, N
28
29 18.44.

30
31 **1-(3-Amino-1H-1,2,4-triazol-5-yl)-N-(4-cyclopropylphenethyl)-N-methylpiperidin-4-amine (7p)**.

32
33 The title compound was prepared by a similar procedure as that used for **7a** and purified by
34
35 crystallization from acetonitrile to give **7p** (195 mg, 62%), mp 108-110°C. LC-MS (ES+): RT 2.0 min,
36
37 m/z 341.35 $[M+H]^+$. 1H NMR (700 MHz, DMSO- d_6 + D_2O) δ 7.04 (d, $J = 8.0$ Hz, 2H), 6.93 (d, $J = 8.0$
38
39 Hz, 2H), 3.75 (d, $J = 11.8$ Hz, 2H), 2.63 – 2.53 (m, 7H), 2.21 (s, 3H), 1.81 (ddd, $J = 13.4, 8.4, 4.9$ Hz,
40
41 1H), 1.66 (d, $J = 12.2$ Hz, 2H), 1.39 – 1.28 (m, 2H), 0.90 – 0.82 (m, 2H), 0.60 – 0.50 (m, 2H).
42
43 Elemental analysis calculated (%) for $C_{19}H_{28}N_6$: C 67.03, H 8.29, N 24.68. Found: C 66.98, H 8.23, N
44
45 24.41.

46
47 **1-(3-Amino-1H-1,2,4-triazol-5-yl)-N-(4-(tert-butyl)phenethyl)-N-methylpiperidin-4-amine (7r)**.

48
49 The title compound was prepared by a similar procedure as that used for **7a** and purified by
50
51 crystallization from acetonitrile to give **7r** (160 mg, 63%), mp 147-148°C. LC-MS (ES+): RT 3.6 min,
52
53 m/z 357.4 $[M+H]^+$. 1H NMR (700 MHz, DMSO- d_6 + D_2O) δ 7.32 (d, $J = 8.4$ Hz, 2H), 7.21 (d, $J = 8.4$
54
55 Hz, 2H), 3.82 (d, $J = 12.6$ Hz, 2H), 3.56 – 3.40 (m, 1H), 3.30 (td, $J = 12.1, 5.0$ Hz, 1H), 3.18 (td, $J =$
56
57
58
59
60

12.1, 5.3 Hz, 1H), 3.09 – 2.80 (m, 4H), 2.75 (s, 3H), 2.04-1.98 (m, 2H), 1.68 (dtd, $J = 32.9, 12.1, 8.4$ Hz, 2H), 1.22 (s, 9H). HRMS calculated for $C_{20}H_{33}N_6 [M+H]^+$ 357.2761, found 357.2744.

1-(3-Amino-1H-1,2,4-triazol-5-yl)-N-(2,4-dichlorophenethyl)-N-methylpiperidin-4-amine (7s).

The title compound was prepared by a similar procedure as that used for **7a** and purified by crystallization from acetonitrile to give **7s** (33 mg, 38%), mp 234-236°C. LC-MS (ES+): RT 2.3 min, m/z 369.2/371.2 $[M+H]^+$. 1H NMR (700 MHz, DMSO- d_6 + D_2O) δ 7.54 (d, $J = 2.2$ Hz, 1H), 7.45 (d, $J = 8.3$ Hz, 1H), 7.37 (dd, $J = 8.3, 2.2$ Hz, 1H), 3.91 – 3.83 (m, 2H), 3.55 – 3.49 (m, 1H), 3.26 (bs, 2H), 3.17 – 3.11 (m, 2H), 2.97 – 2.90 (m, 2H), 2.81 (s, 3H), 2.09 – 2.03 (m, 2H), 1.78 – 1.66 (m, 2H). HRMS calculated for $C_{16}H_{23}Cl_2N_6 [M+H]^+$ 369.1356, found 369.1362.

Synthesis of 1-(3-Amino-1H-1,2,4-triazol-5-yl)-N-(4-bromobenzyl)piperidine-4-carboxamide dihydrochloride (10).

Step 1: Synthesis of *tert-Butyl 4-((4-bromobenzyl)carbamoyl)piperidine-1-carboxylate (9)*. The title compound was prepared by a similar procedure as that used for **3** to give **9** (150 mg, 42%). LC-MS (ES+): RT 5.5 min, m/z 397.1/399.1 $[M+H]^+$. 1H NMR (700 MHz, $CDCl_3$) δ 7.49 – 7.45 (m, 2H), 7.17 – 7.13 (m, 2H), 5.80 (bs, 1H), 4.41 (d, $J = 5.8$ Hz, 2H), 4.16 (bs, 2H), 2.76 (bs, 2H), 2.27 (tt, $J = 11.6, 3.8$ Hz, 1H), 1.87 – 1.80 (m, 2H), 1.67 (qd, $J = 12.2, 4.4$ Hz, 2H), 1.47 (s, 9H).

Step 2: Synthesis of *1-(3-Amino-1H-1,2,4-triazol-5-yl)-N-(4-bromobenzyl)piperidine-4-carboxamide hydrochloride (10)*. The title compound was prepared by a similar procedure as that used for **4** (step 2) to give **10** (53 mg, 37%), mp 224-226°C. LC-MS (ES+): RT 3.7 min, m/z 379.1/381.1 $[M+H]^+$. 1H NMR (700 MHz, DMSO- d_6) δ 8.43 (t, $J = 6.0$ Hz, 1H), 7.57 – 7.39 (m, 2H), 7.29 – 7.11 (m, 2H), 4.21 (d, $J = 6.0$ Hz, 2H), 3.77 (d, $J = 12.8$ Hz, 2H), 2.95 (t, $J = 12.8$ Hz, 2H), 2.45 – 2.37 (m, 1H), 1.80 – 1.72 (m, 2H), 1.65 – 1.52 (m, 2H). HRMS calculated for $C_{15}H_{20}BrN_6O [M+H]^+$ 379.0876, found 379.0868.

1-(1-(3-Amino-1H-1,2,4-triazol-5-yl)piperidin-4-yl)-3-(4-bromophenyl)urea (13a).

Step 1: Synthesis of *tert-Butyl 4-(3-(4-bromophenyl)ureido)piperidine-1-carboxylate (12a)*. To a solution of 4-bromoaniline (0.94 g, 5.46 mmol) in toluene was added diisopropylethylamine (1 mL, 5.46 mmol) and the mixture was cooled in ice-bath. A 20% solution of $COCl_2$ (3.2 mL, 6.58 mmol) in toluene was added in one portion. Bath was removed and after 40 min at rt TLC chloroform/methanol

9/1 showed no 4-bromoaniline remaining. The reaction mixture was concentrated to dryness, dissolved in dichloromethane, diisopropylethylamine (3 mL, 16.44 mmol) and 1-Boc-4-aminopiperidine (1.09 g, 5.48 mmol) were added and the reaction was stirred at rt overnight. TLC and LC-MS indicated reaction was completed. The reaction was diluted with dichloromethane, washed with 2 M HCl, 1 M NaOH, brine, dried over MgSO₄ and concentrated. Crystallization from ethyl acetate/ hexane gave pure product **12a** as white solid (1 g, 52 %). LC-MS (ES+): RT 5.6 min, m/z 398.1/400.1 [M+H]⁺. ¹H NMR (700 MHz, CDCl₃) δ 7.43 – 7.37 (m, 2H), 7.27 – 7.19 (m, 2H), 6.77 (s, 1H), 4.90 (d, *J* = 7.8 Hz, 1H), 4.02 (bs, 2H), 3.84 (tdt, *J* = 11.3, 8.0, 4.1 Hz, 1H), 2.89 (t, *J* = 12.6 Hz, 2H), 2.01 – 1.84 (m, 2H), 1.48 (s, 9H), 1.28 – 1.24 (m, 2H).

Step 2: *1-(1-(3-Amino-1H-1,2,4-triazol-5-yl)piperidin-4-yl)-3-(4-bromophenyl)urea (13a)*. The title compound was prepared by a similar procedure as that used for molecule **4** (step 2) and purified by crystallization from acetonitrile to give **13a** (150 mg, 54%), mp 230-231°C. LC-MS (ES+): RT 3.2 min, m/z 380.4/ 382.4 [M+H]⁺. ¹H NMR (700 MHz, DMSO-d₆) δ 8.43 (s, 1H), 7.38 – 7.31 (m, 4H), 6.20 (d, *J* = 7.7 Hz, 1H), 5.51 (bs, 2H), 3.68 – 3.62 (m, 2H), 3.63 – 3.55 (m, 1H), 2.81 (t, *J* = 11.6 Hz, 2H), 1.82 – 1.68 (m, 2H), 1.44 – 1.28 (m, 2H). HRMS calculated for C₁₄H₁₉BrN₇O [M+H]⁺ 380.0829, found 380.0822.

N-(1-(3-Amino-1H-1,2,4-triazol-5-yl)piperidin-4-yl)-2-(4-bromophenyl)acetamide (13b).

Step 1: *tert-Butyl 4-(2-(4-bromophenyl)acetamido)piperidine-1-carboxylate (12b)*. To a stirred solution of diisopropylethylamine (0.43 mL, 2.5 mmol) in dichloromethane (15 mL) were added 1-Boc-4-aminopiperidine (220 mg, 1.1 mmol) and 4-bromophenylacetic acid (215 mg, 1 mmol). After 5 min TBTU (385 mg, 1.2 mmol) was added and the stirring was continued for 3h. The mixture reaction was diluted with dichloromethane (15 mL) and washed with 0.5 M HCl and with brine. An organic layer was dried over MgSO₄ and solvent was removed in vacuo. The crude residue was purified by column chromatography (1% methanol in dichloromethane) to afford title compound **12b** as off-white solid (370 mg, 93%). LC-MS (ES+): RT 5.4 min, m/z 419.1/421.1 [M+Na]⁺. ¹H NMR (700 MHz, CDCl₃) δ 7.47 (d, *J* = 8.4 Hz, 2H), 7.13 (d, *J* = 8.4 Hz, 2H), 5.20 (d, *J* = 7.6 Hz, 1H), 4.01 - 3.87 (m, 3H), 3.49 (s, 2H), 2.84 – 2.80 (m, 2H), 1.86 – 1.83 (m, 2H), 1.43 (s, 9H), 1.20 (qd, *J* = 12.5, 4.4 Hz, 2H).

1
2
3 Step 2: Synthesis of *N*-(1-(3-Amino-1*H*-1,2,4-triazol-5-yl)piperidin-4-yl)-2-(4-bromophenyl)acetamide
4 (13b). The title compound was prepared by a similar procedure as that used for molecule 4 (step 2)
5 and purified by crystallization from acetonitrile to give 13b (246 mg, 48%), mp 228-229°C. LC-MS
6 (ES+): RT 3.4 min, m/z 379.1/ 381.1 [M+H]⁺. ¹H NMR (700 MHz, DMSO-d₆ + D₂O) δ 7.44 (d, *J* =
7 8.3 Hz, 2H), 7.17 (d, *J* = 8.3 Hz, 2H), 3.64 – 3.58 (m, 3H), 3.33 (s, 2H), 2.79 – 2.74 (m, 2H), 1.67 –
8 1.64 (m, 2H), 1.37 – 1.26 (m, 2H). Elemental analysis calculated (%) for C₁₅H₁₉BrN₆O: C 47.50, H
9 5.05, N 22.16. Found: C 47.43, H 4.96, N 22.04.

10
11
12
13
14
15
16 **N-(1-(3-Amino-1*H*-1,2,4-triazol-5-yl)piperidin-4-yl)-1-(4-bromophenyl)methanesulfonamide**
17 (15a).

18
19 Step 1: Synthesis of *tert*-Butyl 4-((4-bromophenyl)methylsulfonamido)piperidine-1-carboxylate (14a).
20 To a stirred solution of 1-Boc-4-aminopiperidine (200 mg, 1 mmol) and diisopropylethylamine (0.26
21 mL, 1.5 mmol) in dichloromethane (3 mL) was added 4-bromobenzylsulfonyl chloride (270 mg, 1
22 mmol). A whole reaction mixture was stirred at ambient temperature overnight, afterwards it was
23 diluted with dichloromethane (10 mL) and washed twice with water. An organic layer was dried over
24 MgSO₄ and the solvent was removed in vacuo. The crude residue was purified by column
25 chromatography (0.5% methanol in dichloromethane) to afford title compound 14a as off-white solid
26 (190 mg, 45%). LC-MS (ES+): RT 5.7 min, m/z 433.0/435.0 [M+H]⁺. ¹H NMR (700 MHz, CDCl₃) δ
27 7.53 (d, *J* = 8.4 Hz, 2H), 7.28 (d, *J* = 8.4 Hz, 2H), 4.20 (s, 2H), 4.00 - 3.94 (m, 3H), 3.28 – 3.23 (m,
28 1H), 2.79 – 2.75 (m, 2H), 1.89 – 1.86 (m, 2H), 1.45 (s, 9H), 1.33 (qd, *J* = 12.1, 4.1 Hz, 2H).

29
30
31
32
33
34 Step 2: Synthesis of *N*-(1-(3-Amino-1*H*-1,2,4-triazol-5-yl)piperidin-4-yl)-1-(4-
35 bromophenyl)methanesulfonamide (15a). The title compound was prepared by a similar procedure as
36 that used for 4 (step 2) and crystallized from acetonitrile to give 15a as monohydrate (100 mg, 55%),
37 mp 174-176°C. LC-MS (ES+): RT 3.7 min, m/z 415.1/417.1 [M+H]⁺. ¹H NMR (700 MHz, DMSO-d₆
38 + D₂O) δ 7.52 (d, *J* = 8.4 Hz, 2H), 7.32 (d, *J* = 8.4 Hz, 2H), 4.27 (s, 2H), 3.66 (dt, *J* = 13.4, 3.4 Hz,
39 2H), 3.18 (ddt, *J* = 13.0, 6.7, 3.5 Hz, 1H), 2.75 – 2.68 (m, 2H), 1.75 (dt, *J* = 11.0, 2.9 Hz, 2H), 1.44 –
40 1.36 (m, 2H). Elemental analysis calculated (%) for C₁₄H₁₉BrN₆O₂S*H₂O: C 38.81, H 4.89, N 19.39, S
41 7.40. Found: C 38.82, H 5.01, N 19.30, S 7.76.

N-(1-(3-Amino-1H-1,2,4-triazol-5-yl)piperidin-4-yl)-1-(4-bromophenyl)-N-methylmethanesulfonamide hydrochloride (15b).

Step 1: Synthesis of *tert-Butyl 4-(1-(4-bromophenyl)-N-methylmethanesulfonamido)piperidine-1-carboxylate (14b)*. The title compound was prepared by a similar procedure as that used for **14a** by substituting 1-Boc-4-aminopiperidine with 1-Boc-4-(methylamino)piperidine to give **14b** (150 mg, 42%). LC-MS (ES+): RT 6.1 min, m/z 447.2/449.2 [M+H]⁺. ¹H NMR (700 MHz, CDCl₃) δ 7.52 (d, *J* = 8.4 Hz, 2H), 7.27 (d, *J* = 8.4 Hz, 2H), 4.17 – 4.11 (m, 2H), 4.14 (s, 2H), 3.64 (tt, *J* = 11.9, 4.1 Hz, 1H), 2.66 – 2.61 (m, 2H), 2.63 (s, 3H), 1.58 – 1.52 (m, 2H), 1.49 – 1.46 (m, 2H), 1.45 (s, 9H).

Step 2: Synthesis of *N-(1-(3-Amino-1H-1,2,4-triazol-5-yl)piperidin-4-yl)-1-(4-bromophenyl)-N-methylmethanesulfonamide hydrochloride (15b)*. The title compound was prepared by a similar procedure as that used for **4** (step 2) and purified by preparative HPLC to give **15b** (48 mg, 42%), mp 138-139°C. LC-MS (ES+): RT 4.1 min, m/z 429.1/431.1 [M+H]⁺. ¹H NMR (700 MHz, DMSO-d₆) δ 7.60 (d, *J* = 8.5 Hz, 2H), 7.37 (d, *J* = 8.5 Hz, 2H), 4.45 (s, 2H), 3.83 (bd, *J* = 12.2 Hz, 2H), 3.73 (ddd, *J* = 15.7, 7.9, 3.8 Hz, 1H), 2.97 (bt, *J* = 12.9 Hz, 2H), 2.62 (s, 3H), 1.71 (qd, *J* = 12.4, 4.3 Hz, 2H), 1.58 – 1.56 (m, 2H). Elemental analysis calculated (%) for C₁₅H₂₁BrN₆O₂S*HCl*H₂O: C 37.24, H 5.00, N 17.37, S 6.63. Found: C 37.28, H 4.77, N 17.40, S 6.69.

5-(4-(((4-Bromobenzyl)(methyl)amino)methyl)piperidin-1-yl)-1H-1,2,4-triazol-3-amine trihydrochloride (18a).

Step 1: Synthesis of *tert-Butyl 4-(((4-bromobenzyl)(methyl)amino)methyl)piperidine-1-carboxylate (17a)*. The title compound was prepared by a similar procedure as that used for **6a** to give **17a** (270 mg, 72%). LC-MS (ES+): RT 4.5 min, m/z 397.1/399.1 [M+H]⁺. ¹H NMR (700 MHz, CDCl₃) δ 7.44 (d, *J* = 8.3 Hz, 2H), 7.20 (d, *J* = 8.3 Hz, 2H), 4.08 (bs, 2H), 3.42 (s, 2H), 2.70 (bs, 2H), 2.19 (bd, *J* = 7.2 Hz, 2H), 2.18 (s, 3H), 1.77 (bd, *J* = 12.5 Hz, 1H), 1.68 -1.64 (m, 1H), 1.47 (s, 9H), 1.06 – 1.00 (m, 2H).

Step 2: Synthesis of *5-(4-(((4-Bromobenzyl)(methyl)amino)methyl)piperidin-1-yl)-1H-1,2,4-triazol-3-amine trihydrochloride (18a)*. The title compound was prepared by a similar procedure as that used for **4** (step 2) and purified by preparative HPLC to give **18a** as hydrochloride salt (70 mg, 27%), mp 68-70°C. LC-MS (ES+): RT 0.5 min, m/z 379.2/ 381.2 [M+H]⁺. ¹H NMR (700 MHz, DMSO-d₆ + D₂O) δ

7.68 – 7.62 (m, 2H), 7.47 – 7.44 (m, 2H), 4.36 – 4.27 (m, 1H), 4.23 – 4.14 (m, 1H), 3.65 (d, $J = 12.8$ Hz, 2H), 2.99 – 2.85 (m, 4H), 2.68 (s, 3H), 2.08 – 2.00 (m, 1H), 1.82 – 1.65 (m, 2H), 1.28 – 1.02 (m, 2H). HRMS calculated for $C_{16}H_{24}BrN_6$ $[M+H]^+$ 379.1240, HRMS found: 379.1230

Synthesis of *N*-((1-(3-Amino-1*H*-1,2,4-triazol-5-yl)piperidin-4-yl)methyl)-4-bromobenzamide (**18b**).

Step 1: Synthesis of *tert*-Butyl 4-((4-bromobenzamido)methyl)piperidine-1-carboxylate (**17b**). The title compound was prepared by a similar procedure as that used for **3** to give **17b** (350 mg, 94%). LC-MS (ES+): RT 5.6 min, m/z 397.0/399.0 $[M+H]^+$. 1H NMR (700 MHz, $CDCl_3$) δ 7.65 (d, $J = 8.7$ Hz, 2H), 7.59 (d, $J = 8.7$ Hz, 2H), 6.18 (bs, 1H), 4.16 (bs, 2H), 3.38 (bs, 2H), 2.72 (bs, 2H), 1.85 – 1.72 (m, 1H), 1.77 – 1.69 (m, 2H), 1.47 (s, 9H), 1.24 – 1.18 (m, 2H).

Step 2: Synthesis of *N*-((1-(3-Amino-1*H*-1,2,4-triazol-5-yl)piperidin-4-yl)methyl)-4-bromobenzamide (**18b**). The title compound was prepared by a similar procedure as that used for **4** (step 2) and purified by crystallization from acetonitrile to give **18b** (128 mg, 38%), mp 222-224°C. LC-MS (ES+): RT 3.4 min, m/z 379.1/ 381.1 $[M+H]^+$. 1H NMR (700 MHz, $DMSO-d_6 + D_2O$) δ 7.72 (d, $J = 8.5$ Hz, 2H), 7.65 (d, $J = 8.5$ Hz, 2H), 3.72 (d, $J = 12.7$ Hz, 2H), 3.14 (d, $J = 6.8$ Hz, 2H), 2.65 – 2.55 (m, 2H), 1.71 – 1.57 (m, 3H), 1.14 (tt, $J = 11.9, 6.3$ Hz, 2H). Elemental analysis calculated (%) for $C_{15}H_{19}BrN_6O \cdot 0.5H_2O$: C 46.40, H 5.19, N 21.65. Found: C 46.25, H 4.82, N 21.60.

X-ray Crystallography:

Early to crystallization, the construct corresponding to the catalytic domain (residues 1–386; hCHIT1) was produced and purified as described²². For crystallization of the apo form of the this construct, the protein was concentrated to 9 mg/ml in 10 mM HEPES, 150 mM NaCl pH 7.5 buffer and crystals were grown by the hanging-drop vapor-diffusion method at 17°C. Drops containing 1.5 μ L of protein solution were mixed with an equal volume of the precipitant solution consisting of 25% (w/v) polyethylene glycol (PEG) 3350, 200 mM potassium sodium tartrate (PST) at pH 7.2. The crystals reached maximum dimensions after 4–6 days of equilibration against 500 μ L of the reservoir solution. Soaking experiments were used to obtain crystals of the hCHIT1–inhibitor complexes. Native crystals of hCHIT1 catalytic domain were transferred to 10 μ L of a reservoir solution containing 5 mM of each

1
2 inhibitor and 2.5 % DMSO. Soaking time was 1 hour for each compound. All soaked crystals were
3 cryocooled in liquid nitrogen using a solution containing 35% PEG 3350, 200 mM PST.
4

5
6 Data Collection. X-ray diffraction data were collected on the X06DA (PXIII) beamline at the Swiss
7 Light Source (SLS), Villigen, Switzerland. X-ray diffraction data were collected at 1.35 Å, 1.27 Å and
8 1.44 Å for the complexes hCHIT1-compound **7a**, **7g**, and **7i** respectively. The crystals belong to the
9 same space group P2₁2₁2 with unit cell parameters a=85 Å b=106 Å c=42 Å. All data sets were
10 integrated, merged and scaled using HKL-2000.²⁷ The structures were solved by molecular
11 replacement with Phaser²⁸ using the coordinates of the native structure of the same protein as an
12 initial search model (PDB ID: 4WJX)²². The model was improved by alternating cycles of manual
13 model building using Coot²⁹ with refinement using REFMAC5³⁰ and PHENIX³¹ assessed with
14 MolProbity³². The stereochemical quality of the final model for the three complexes are included in
15 Table 5.
16

17
18 The atomic coordinates have been deposited in the Protein Data Bank (PDB IDs: 5NR8 CHIT1-7a,
19 5NRF CHIT1-7i, 5NRA CHIT1-7g and will be released upon publication. The inhibitor binding sites
20 were analyzed using Coot²⁹ while figures were generated with the PyMOL Molecular Graphics
21 System (Delano Scientific LLC).
22
23
24
25
26
27
28
29
30
31
32
33
34
35
36
37
38
39
40
41
42
43
44
45
46
47
48
49
50
51
52
53
54
55
56
57
58
59
60

Table 5. Data collection and refinement statistics

	hCHIT1-Compound 7a	hCHIT1-Compound 7g	hCHIT1-Compound 7i
Wavelength (Å)	0.8	0.8	0.8
Resolution range (Å)	30.09 - 1.349 (1.397 - 1.349)	17.59 - 1.267 (1.313 - 1.267)	28.93 - 1.447 (1.499 - 1.447)
Space group	P 2 ₁ 2 ₁ 2	P 2 ₁ 2 ₁ 2	P 2 ₁ 2 ₁ 2
Unit cell	85.9 106.0 42.15	85.45 105.6 42.13	85.6 105.99 42.24
Total reflections	531590	590678	381836
Unique reflections	83374 (8047)	100288 (9387)	67782 (6543)
Multiplicity	6.4 (6.4)	5.9 (6.1)	5.9 (5.3)
Completeness (%)	97.44 (95.50)	98.49 (93.41)	97.70 (95.48)
Mean I/sigma(I)	34.08 (3.0)	25.9 (2.9)	26.32 (3.11)
Wilson B-factor	14.19	11.74	13.30
R-sym	2.8% (52.4%)	5.8% (53.0%)	5.7% (55.3%)
R-factor	13.21% (17.44%)	13.69% (18.66%)	14.40% (15.99%)
R-free	15.60% (21.86%)	16.30% (22.25%)	16.93% (20.23%)
Number of atoms	6550	3472	3396
macromolecules	3146	3061	3155
ligands	65	32	41
water	222	379	200
Protein residues	377	377	377
RMS (bonds)	0.009	0.006	0.008
RMS (angles)	1.31	1.12	1.16
Ramachandran favored (%)	98	99	99
Ramachandran outliers (%)	0	0	0
Clashscore	5.95	4.51	5.40
Average B-factor	16.90	15.30	16.80
macromolecules	16.10	13.60	16.20
ligands	26.30	11.60	16.60
solvent	25.80	28.70	26.00

Biological Methods (In Vitro)

Enzymatic assays – IC₅₀ determination towards human and mouse AMCCase and human and mouse CHIT1

Human and mouse AMCCase and human and mouse CHIT1 recombinant proteins were produced in CHO-K1 cells after transient transfection with plasmid coding full-length protein with C-terminal His-tag. The proteins were purified by nickel-affinity chromatography. Chitinolytic activity of recombinant enzymes was measured using standard assay as previously described^{12, 13}. For determination of enzymatic activity 103 μM 4-methylumbelliferyl β-D-N,N' diacetylchitobioside hydrate and 5.2 ng per well of hAMCCase, 46 μM 4-methylumbelliferyl β-D-N,N'-diacetylchitobioside hydrate and 3 ng per well of mAMCCase, 5 μM 4-methylumbelliferyl β-D-N,N',N'' triacetylchitotrioside and 0.2 ng per well of hCHIT1 or 20 μM 4-methylumbelliferyl β-D-N,N',N'' triacetylchitotrioside and 2 ng per well of mCHIT1 were used. Appropriate substrate, enzyme and varying concentrations of compounds in assay buffer (0.1 M citrate, 0.2 M dibasic phosphate, 1 mg/mL BSA) were incubated in a 96-well black microtiter plate with shaking in the dark, at 37°C for 60 minutes followed by addition of stop solution (0.3 M glycine/NaOH Buffer, pH 10.5). Substrate hydrolysis product - 4-methylumbelliferone was measured fluorometrically using Spark M10 (Tecan) microplate reader (excitation 355 nm/emission 460 nm). IC₅₀ values of all inhibitors against AMCCase and CHIT1 were determined from dose-response sigmoidal curves of the % of inhibition vs. log (inhibitor concentration) using GraphPad Prism v. 6.0. Experiments were performed in duplicate or triplicate.

Enzymatic assays - Ki determination towards both human and mouse AMCCase and CHIT1

For experimental determination of the Ki, recombinant enzyme (5.2 ng/well hAMCCase or hCHIT1, 3 ng/well mAMCCase, 5 ng/well mCHIT1), varying concentrations of substrate 4-methylumbelliferyl β-D-N,N'-diacetylchitobioside hydrate or 4-methylumbelliferyl β-D-N,N',N'' triacetylchitotrioside and varying concentrations of compound in citrate buffer, pH 5.2 were incubated in a black microtiter plate, in the dark, at 37°C for 60 minutes followed by addition of stop solution. Substrate hydrolysis product - 4-methylumbelliferone was measured fluorometrically using Spark M10 (Tecan) microplate

1
2
3 reader (excitation 355 nm/emission 460 nm). K_i values were derived experimentally using
4
5 Lineweaver-Burk plot.
6
7

8 **hERG Binding assay**

9
10 To characterize the affinity of compounds to the hERG channel, the Predictor(TM) hERG
11
12 Fluorescence Polarisation Assay Kit (Invitrogen) was used according to manufacturer's protocol²⁵.
13
14
15

16 **Biological Methods (In Vivo)**

17
18 All in vivo experiments were performed in accordance with the guidelines of the Institute for Animal
19
20 Care and Use Committee in Poland and all protocols were approved by Local Ethic Committee,
21
22 Warsaw, Poland.
23
24
25

26 **Pharmacokinetic measurements:** The pharmacokinetic properties of compounds were evaluated in
27
28 female BALB/c mice following single intravenous bolus or oral administrations. Compounds were
29
30 prepared in a 30% PEG400/70% water vehicle for intravenous bolus and oral administrations at 2
31
32 mL/kg or 5 mL/kg, respectively, and administered to 2 mice/group/timepoint with samples collected
33
34 out to 24 h post-dose. Blood collection was performed by cardiac puncture under anesthesia with
35
36 sampling of blood into K_2EDTA anticoagulant tubes, followed by centrifugation to obtain plasma.
37
38 Samples were stored frozen at $-20^\circ C$ or lower prior to compound extraction and LC/MS/MS analysis.
39
40 Pharmacokinetic parameters were calculated by standard noncompartmental modeling from the
41
42 systemic plasma concentration-time profiles for each compound.
43
44
45

46 **HDM Mouse Model of Allergic Pulmonary Inflammation**

47
48 Determination of the therapeutic efficacy of compound **7f** in comparison to high dose dexamethasone
49
50 treatment was carried out in 3 week exposure to HDM-induced mouse model of allergic airway
51
52 inflammation. Briefly, 3 groups (n=8; HDM with or without **7f** or dexamethasone treatment) of age-
53
54 matched 8-week-old female BALB/c mice (Charles River, Germany) were subjected to intranasal
55
56 exposure of 40 μg of HDM extract (Greer, Lenoir, NC) in 25 μL PBS solution 5 times per week for 19
57
58
59
60

1
2
3 days. In addition, naive mice were subjected to PBS intranasal challenges at times of HDM challenges
4 (n=8). Selective AMCase inhibitor, compound **7f** was administered orally (20 $\mu\text{L/g}$) at a dose of 30
5 mg/kg starting from day 7 onwards representing therapeutic treatment scheme as compared to vehicle-
6 treated controls (vehicle: (EtOH : glucose : water (40 : 10 : 5 : 45 v/v). Dexamethasone (Dexaven[®])
7 was administered by intraperitoneal injection at a dose of 10 mg/kg in a therapeutic treatment regimen
8 (from day 7 onwards) similarly to **7f**.
9
10
11
12
13

14 15 16 **Assessment of pulmonary inflammation**

17
18 The mice were allowed to rest 24h post last HDM challenge and drug dosing and on day 19 animals
19 were euthanized by lethal morbital[®] injection (sodium pentobarbital 26.7 mg/mL, pentobarbital 133.3
20 mg/mL; Biovet, Poland), followed by the collection of BALF for subsequent assessment of pulmonary
21 inflammation. Briefly, lungs were washed via trachea using 1 mL of PBS. The BAL was centrifuged
22 (10 min, 2000 rpm, 4°C). Supernatant was collected and stored at -80°C for further analysis
23 (chitinolytic activity) and cells pellet was resuspended in 300 μL of PBS and subsequently used for
24 manual cell counting and FACS analysis for leukocyte subpopulations identification. Total BALF
25 cells were counted manually using Buerker's chamber and were further characterized with flow
26 cytometry (FACSAria, BD) using the relevant antibody cocktail to discriminate leukocyte (CD45
27 positive) subpopulations such as eosinophils (Siglec F positive, CD11c negative), macrophages
28 (Siglec F positive, CD11c positive), neutrophils (Siglec F negative, Gr1 positive), B cells (CD19
29 positive, Siglec F negative) and T cells (CD3 positive, CD19 negative).
30
31
32
33
34
35
36
37
38
39
40
41
42
43

44 **Chitinolytic activity in BAL fluid**

45
46 The BAL fluid was stored at -80°C prior to measurement of the chitinolytic activity as previously
47 described². For determination of enzymatic activity 1 μL of BAL fluid and 196 μM 4-
48 Methylumbelliferyl B-D-N,N' diacetylchitobioside hydrate in assay buffer (0.1 M citrate, 0.2 M
49 dibasic phosphate, 1 mg/ml BSA pH 6.0) were incubated in a 96-well black microtiter plate with
50 shaking in the dark, at 37°C for 60 minutes followed by addition of stop solution (0.3 M
51 glycine/NaOH Buffer, pH 10.5). Substrate hydrolysis product - 4-methylumbelliferone was measured
52
53
54
55
56
57
58
59
60

1
2 fluorometrically using Spark M10 (Tecan) microplate reader (excitation 355 nm/emission 460 nm).
3
4 For the standard curve, serial dilutions of 4-methylumbelliferone in citrate buffer pH 6.0 were used.
5
6 Experiments were performed in duplicate.
7
8
9

10 **Total plasma IgE levels**

11
12 Blood was collected from the vena hepaticae and centrifuged 10 min, 2000 g in rt. Plasma was
13
14 collected and then frozen in -80°C. Total plasma IgE level was quantified using ELISA (eBioscience)
15
16 according to manufacturer's protocol.
17
18
19

20 **AUTHOR INFORMATION**

21
22 Corresponding Author

23
24 *Phone: +48 (22) 552 67 24; E-mail: a.golebiowski@oncoarendi.com

25
26 Current address:

27
28 # LAM Therapeutics, 530 Whitfield St., Guilford CT 06437, USA

29
30 ¶ Selvita S.A., Park Life Science, Bobrzynskiego 14, 30-348 Cracow, Poland.

31
32 // Yale Center for Molecular Discovery, 300 Heffernan Dr. #B27/116D, West Haven, CT 06516, USA

33
34 ‡ Laboratoire d'Ingénierie des Systèmes Macromoléculaires, Institut de Microbiologie de la
35
36 Méditerranée, Aix-Marseille Université, CNRS UMR7255, Marseille, France.

37
38 & AFMB, Aix Marseille Université, CNRS UMR 7257, 13288, Marseille, France and Laboratoire
39
40 d'Ingénierie des Systèmes Macromoléculaires, Institut de Microbiologie de la Méditerranée, Aix-
41
42 Marseille Université, CNRS UMR7255, Marseille, France.
43
44
45

46 **AUTHORS CONTRIBUTIONS**

47
48 The manuscript was written through contributions of all authors. All authors have given approval to
49
50 the final version of the manuscript.
51
52
53

54 **NOTES**

1
2
3 The authors declare the following competing financial interest(s): Some of the authors are current
4 employees of OncoArendi Therapeutics and own company stocks.
5
6
7

8 **ACKNOWLEDGMENTS**

9
10 Studies were supported by two projects - "Selective inhibitors of acidic mammalian chitinase
11 (AMCase) as potential therapy for asthma" - acronym AMCase, co-financed by the National Centre
12 for Research and Development in the framework of Innovative Economy Operational Programme and
13
14 "Preclinical research and clinical trials of a first-in-class development candidate in therapy of asthma
15 and inflammatory bowel disease" - acronym IBD, co-financed by the National Centre for Research
16 and Development in the framework of European Funds Smart Growth.
17
18

19 We thank the IGBMC Structural Genomics Platform staff (in particular Dr. Alastair McEwen and
20 Pierre Poussin-Courmontagne). The crystallographic experiments were performed on the X06DA
21 beamline at the Swiss Light Source synchrotron, Paul Scherrer Institut, Villigen, Switzerland. We
22 thank in particular Dr Vincent Olieric and Dr Martin Fuchs for their help in data collection. This work
23 has been funded by the CNRS, the INSERM, the Université de Strasbourg, the Région Alsace, the
24 Hôpital Civil de Strasbourg, Instruct (part of the European Strategy Forum of Research Infrastructures;
25 ESFRI) and the French Infrastructure for Integrated Structural Biology (FRISBI).
26
27
28
29
30
31
32
33
34
35
36
37

38 **ABBREVIATIONS USED**

39
40 HDM, house dust mite; AMCase, acidic mammalian chitinase; hAMCase, human AMCase;
41 mAMCase, mouse AMCase; CHIT1, chitotriosidase; hCHIT1, human CHIT1; mCHIT1, mouse
42 CHIT1; YKL-40, chitinase-3-like protein 1 (CHI3L1), also known as YKL-40; BRP-39, mouse breast
43 regression protein 39; YM1, chitinase-3-like protein 3; YM2, chitinase-3-like protein 4; shRNA, small
44 hairpin RNA; IL-13, interleukin 13; OVA, ovalbumin; Th2, type 2 helper T cells; TBTU, N,N,N',N'-
45 tetramethyl-O-(benzotriazol-1-yl)uronium tetrafluoroborate; DIPEA, N,N-diisopropylethylamine; V_{ss} ,
46 steady-state volume of distribution; CL, clearance; AUC_{0-inf} , area under the curve; C_{max} , the peak
47 plasma concentration of a drug after administration; T_{max} , time to reach C_{max} ; LM Stb, liver
48 microsomes stability; BAL, bronchoalveolar lavage; IgE, immunoglobulin E, RT, retention time.
49
50
51
52
53
54
55
56
57
58
59
60

ASSOCIATED CONTENT / SUPPORTING INFORMATION

The Supporting Information is available free of charge on the ACS Publications website at

DOI:

¹H NMR spectra of compounds **3** – **18b**

Molecular formula strings and some data (CSV)

Accession Codes

The atomic coordinates have been deposited in the Protein Data Bank (PDB IDs: 5NR8 CHIT1-7a, 5NRF CHIT1-7i, 5NRA CHIT1-7g) and will be released upon publication.

REFERENCES

1. Lee, C. G.; Da Silva, C. A.; Dela Cruz, C. S.; Ahangari, F.; Ma, B.; Kang, M. J.; He, C. H.; Takyar, S.; Elias, J. A. Role of chitin and chitinase/chitinase-like proteins in inflammation, tissue remodeling, and injury. *Annu. Rev. Physiol.* **2011**, *73*, 479-501.
2. Zhu, Z.; Zheng, T.; Homer, R. J.; Kim, Y. K.; Chen, N. Y.; Cohn, L.; Hamid, Q.; Elias, J. A. Acidic mammalian chitinase in asthmatic Th2 inflammation and IL-13 pathway activation. *Science* **2004**, *304*, 1678-1682.
3. Shen, C. R.; Juang, H. H.; Chen, H. S.; Yang, C. J.; Wu, C. J.; Lee, M. H.; Hwang, Y. S.; Kuo, M. L.; Chen, Y. S.; Chen, J. K.; Liu, C. L. The Correlation between chitin and acidic mammalian chitinase in animal models of allergic asthma. *Int. J. Mol. Sci.* **2015**, *16*, 27371-27377.
4. Cho, W. S.; Kim, T. H.; Lee, H. M.; Lee, S. H.; Lee, S. H.; Yoo, J. H.; Kim, Y. S.; Lee, S. H. Increased expression of acidic mammalian chitinase and chitotriosidase in the nasal mucosa of patients with allergic rhinitis. *Laryngoscope* **2010**, *120*, 870-875.
5. Musumeci, M.; Bellin, M.; Maltese, A.; Aragona, P.; Bucolo, C.; Musumeci, S. Chitinase levels in the tears of subjects with ocular allergies. *Cornea* **2008**, *27*, 168-173.

- 1
2
3 6. Ramanathan, M.; Jr., Lee, W. K.; Lane, A. P. Increased expression of acidic mammalian
4 chitinase in chronic rhinosinusitis with nasal polyps. *Am. J. Rhinol.* **2006**, *20*, 330-335.
5
6
- 7 7. Yang, C. J.,; Liu, Y. K.; Liu, C. L.; Shen, C. N.; Kuo, M. L.; Su, C. C.; Tseng, C. P.; Yen, T.
8 C.; Shen, C. R. Inhibition of acidic mammalian chitinase by RNA interference suppresses ovalbumin-
9 sensitized allergic asthma. *Hum. Gene Ther.* **2009**, *20*, 1597-1606.
10
11
- 12 8. Matsumoto, T.; Inoue, H.; Sato, Y.; Kita, Y.; Nakano, T.; Noda, N.; Eguchi-Tsuda, M.;
13 Moriwaki, A.; Kan-O, K.; Matsumoto, K.; Shimizu, T.; Nagasawa, H.; Sakuda, S.; Nakanishi, Y.
14 Demethylallosamidin, a chitinase inhibitor, suppresses airway inflammation and hyperresponsiveness.
15
16
17
18
19
20
21
22 *Biochem. Biophys. Res. Commun.* **2009**, *390*, 103-108.
- 23 9. Huang, G.; Peng, D.; Mei, X.; Chen, X.; Xiao, F.; Tang, Q. High-efficient synthesis and
24 biological activities of allosamidins. *J. Enzyme Inhib. Med. Chem.* **2015**, *30*, 863-866.
25
26
- 27 10. Hirose, T.; Sunazuka, T.; Omura, S. Recent development of two chitinase inhibitors, Argifin
28 and Argadin, produced by soil microorganisms. *Proc. Jpn. Acad., Ser. B* **2010**, *86*, 85-102.
29
30
- 31 11. Rao, F. V.; Andersen, O. A.; Vora, K. A.; Demartino, J. A.; van Aalten, D. M.
32 Methylxanthine drugs are chitinase inhibitors: investigation of inhibition and binding modes. *Chem.*
33
34
35
36
37
38 *Biol.* **2005**, *12*, 973-980.
- 39 12. Sutherland, T. E.; Andersen, O. A.; Betou, M.; Eggleston, I. M.; Maizels, R. M.; van Aalten,
40 D.; Allen, J. E. Analyzing airway inflammation with chemical biology: dissection of acidic
41 mammalian chitinase function with a selective drug-like inhibitor. *Chem. Biol.* **2011**, *18*, 569-579.
42
43
44
- 45 13. Cole, D. C.; Olland, A. M.; Jacob, J.; Brooks, J.; Bursavich, M. G.; Czerwinski, R.; DeClercq,
46 C.; Johnson, M.; Joseph-McCarthy, D.; Ellingboe, J. W.; Lin, L.; Nowak, P.; Presman, E.; Strand, J.;
47 Tam, A.; Williams, C. M.; Yao, S.; Tsao, D. H.; Fitz, L. J. Identification and characterization of
48 acidic mammalian chitinase inhibitors. *J. Med. Chem.* **2010**, *53*, 6122-6128.
49
50
51
52
- 53 14. Shurin, M. R.; Yanamala, N.; Kisin, E. R.; Tkach, A. V.; Shurin, G. V.; Murray, A. R.;
54 Leonard, H. D.; Reynolds, J. S.; Gutkin, D. W.; Star, A.; Fadeel, B.; Savolainen, K.; Kagan, V. E.;
55
56
57
58
59
60

1
2
3 Shvedova, A. A. Graphene oxide attenuates Th2-type immune responses, but augments airway
4 remodeling and hyperresponsiveness in a murine model of asthma. *ACS Nano* **2014**, *8*, 5585-5599.

7
8 15. Fitz, L. J.; DeClercq, C.; Brooks, J.; Kuang, W.; Bates, B.; Demers, D.; Winkler, A.; Nocka,
9 K.; Jiao, A.; Greco, R. M.; Mason, L. E.; Fleming, M.; Quazi, A.; Wright, J.; Goldman, S.; Hubeau,
10 C.; Williams, C. M. Acidic mammalian chitinase is not a critical target for allergic airway disease.
11 *Am. J. Respir. Cell Mol. Biol.* **2012**, *46*, 71-79.

14
15
16 16. Vannella, K. M.; Ramalingam, T. R.; Hart, K. M.; de Queiroz Prado, R.; Sciruba, J.; Barron,
17 L.; Borthwick, L. A.; Smith, A. D.; Mentink-Kane, M.; White, S.; Thompson, R. W.; Cheever, A. W.;
18 Bock, K.; Moore, I.; Fitz, L. J.; Urban, J. F. Jr.; Wynn, T. A. Acidic chitinase primes the protective
19 immune response to gastrointestinal nematodes. *Nat. Immunol.* **2016**, *17*, 538-544.

22
23
24 17. Kim, L. K.; Morita, R.; Kobayashi, Y.; Eisenbarth, S. C.; Lee, C. G.; Elias, J.; Eynon, E. E.;
25 Flavell, R. A. AMCcase is a crucial regulator of type 2 immune responses to inhaled house dust mites.
26 *Proc. Natl. Acad. Sci. U. S. A.* **2015**, *112*, E2891-E2899.

29
30
31 18. Lee, C. G.; Hartl, D.; Lee, G. R.; Koller, B.; Matsuura, H.; Da Silva, C. A.; Sohn, M. H.;
32 Cohn, L.; Homer, R. J.; Kozhich, A. A.; Humbles, A.; Kearley, J.; Coyle, A.; Chupp, G.; Reed, J.;
33 Flavell, R. A.; Elias, J. A. Role of breast regression protein 39 (BRP-39)/chitinase 3-like-1 in Th2 and
34 IL-13-induced tissue responses and apoptosis. *J. Exp. Med.* **2009**, *206*, 1149-1166.

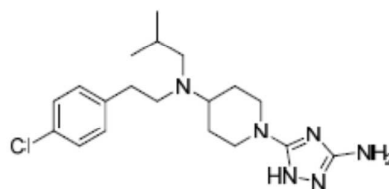
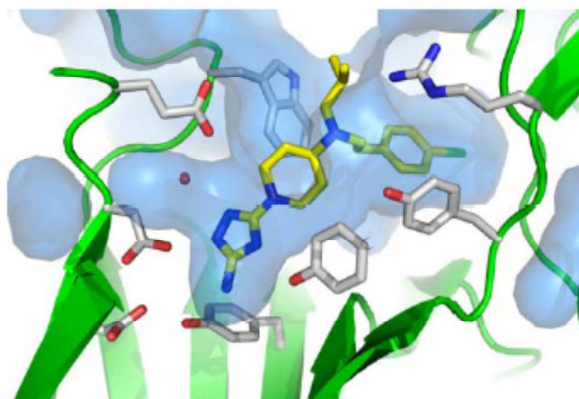
37
38
39 19. Hinks, T. S.; Brown, T.; Lau, L. C.; Rupani, H.; Barber, C.; Elliott, S.; Ward, J. A.; Ono, J.;
40 Ohta, S.; Izuhara, K.; Djukanović, R.; Kurukulaaratchy, R. J.; Chauhan, A.; Howarth, P. H.
41 Multidimensional endotyping in patients with severe asthma reveals inflammatory heterogeneity in
42 matrix metalloproteinases and chitinase 3-like protein 1. *J. Allergy Clin. Immunol.* **2016**, *138*, 61-75.

44
45
46 20. Chupp, G. L.; Lee, C. G.; Jarjour, N.; Shim, Y. M.; Holm, C. T.; He, S.; Dziura, J. D.; Reed,
47 J.; Coyle, A. J.; Kiener, P.; Cullen, M.; Grandsaigne, M.; Dombret, M. C.; Aubier, M.; Pretolani, M.;
48 Elias, J. A. A chitinase-like protein in the lung and circulation of patients with severe asthma. *N. Engl.*
49 *J. Med.* **2007**, *357*, 2016-2027.

- 1
2
3 21. Tomcufcik, A. S.; Meyer, W. E.; Dusza, J. P. 2-(Substituted-1-Piperazinyl)-
4 [1,2,4]triazolo[1,5-a]pyrimidines. U.S. Patent 4,582,833, 1986.
5
6
7 22. Fadel, F.; Zhao, Y.; Cachau, R.; Cousido-Siah, A.; Ruiz, F. X.; Harlos, K.; Howard, E.;
8 Mitschler, A.; Podjarny, A. New insights into the enzymatic mechanism of human chitotriosidase
9 (CHIT1) catalytic domain by atomic resolution X-ray diffraction and hybrid QM/MM. *Acta*
10 *Crystallogr., Sect. D: Struct. Biol.* **2015**, *71*, 1455–1470.
11
12
13 23. Corman, M. L.; Hungerford, W. M.; Golebiowski, A.; Beckett, R. P.; Mazur, M.; Olejniczak,
14 S.; Olczak, J. Substituted Amino Triazoles, and Methods Using Same. US Patent 20160297823,
15 2016.
16
17
18 24. Maron, D. M.; Ames, B. N. Revised methods for the Salmonella mutagenicity test. *Mutat. Res.*
19 **1983**, *113*, 173-215.
20
21
22 25. Piper, D. R.; Duff, S. R.; Eliason, H. C.; Frazee, W. J.; Frey, E. A.; Fuerstenau-Sharp, M.;
23 Jachec, C.; Marks, B. D.; Pollok, B. A.; Shekhani, M. S.; Thompson, D. V.; Whitney, P.; Vogel, K.
24 W.; Hess, S. D. Development of the predictor HERG fluorescence polarization assay using a
25 membrane protein enrichment approach. *Assay Drug Dev. Technol.* **2008**, *6*, 213-223.
26
27
28 26. CEREP Diversity Panel™ composed of 71 binding and 27 enzyme assays (Sept 17, 2017)
29 <http://www.cerep.fr/cerep/users/pages/catalog/profiles/DetailProfile.asp?profile=2121>
30
31
32 27. Otwinowski, Z.; Minor, W. Processing of x-ray diffraction data collected in oscillation mode
33 in methods in enzymology. *Macromol. Crystallogr.* **1997**, *276*, 307–326.
34
35
36 28. McCoy, A. J.; Grosse-Kunstleve, R. W.; Adams, P. D.; Winn, M. D.; Storoni, L. C.; Read, R.
37 J. Phaser crystallographic software. *J. Appl. Crystallogr.* **2007**, *40*, 658–674.
38
39
40 29. Emsley, P.; Lohkamp, B.; Scott, W. G.; Cowtan, K. Features and development of Coot. *Acta*
41 *Crystallogr. Sect. D Biol. Crystallogr.* **2010**, *66*, 486–501.
42
43
44
45
46
47
48
49
50
51
52
53
54
55
56
57
58
59
60

- 1
2
3 30. Murshudov, G. N.; Skubák, P.; Lebedev, A. A.; Pannu, N. S.; Steiner, R. A.; Nicholls, R. A.;
4 Winn, M. D.; Long, F.; Vagin, A. A. REFMAC5 for the refinement of macromolecular crystal
5 structures. *Acta Crystallogr. Sect. D. Biol. Crystallogr.* **2011**, *67*, 355–367.
6
7
8
9 31. Adams, P. D.; Afonine, P. V.; Bunkóczi, G.; Chen, V. B.; Davis, I. W.; Echols, N.; Headd, J.
10 J.; Hung, L.-W.; Kapral, G. J.; Grosse-Kunstleve, R. W.; McCoy, A. J.; Moriarty, N. W.; Oeffner, R.;
11 Read, R. J.; Richardson, D. C.; Richardson, J. S.; Terwilliger, T. C.; Zwart, P. H. PHENIX: A
12 Comprehensive Python-based system for macromolecular structure solution. *Acta Crystallogr. Sect. D.*
13 *Biol. Crystallogr.* **2010**, *66*, 213–221.
14
15
16
17
18
19
20 32. Chen, V. B.; Arendall, W. B.; Headd, J. J.; Keedy, D. A.; Immormino, R. M.; Kapral, G. J.;
21 Murray, L. W.; Richardson, J. S.; Richardson, D. C.; Richardson, D. C. MolProbity: All-atom
22 structure validation for macromolecular crystallography. *Acta Crystallogr. Sect. D. Biol. Crystallogr.*
23 **2010**, *66*, 12–21.
24
25
26
27
28
29
30

Table of Contents Graphic



hAMCase	IC ₅₀ = 14 nM
hCHIT1	IC ₅₀ = 232 nM
mAMCase	IC ₅₀ = 19 nM
mCHIT1	IC ₅₀ = 2955 nM

156x

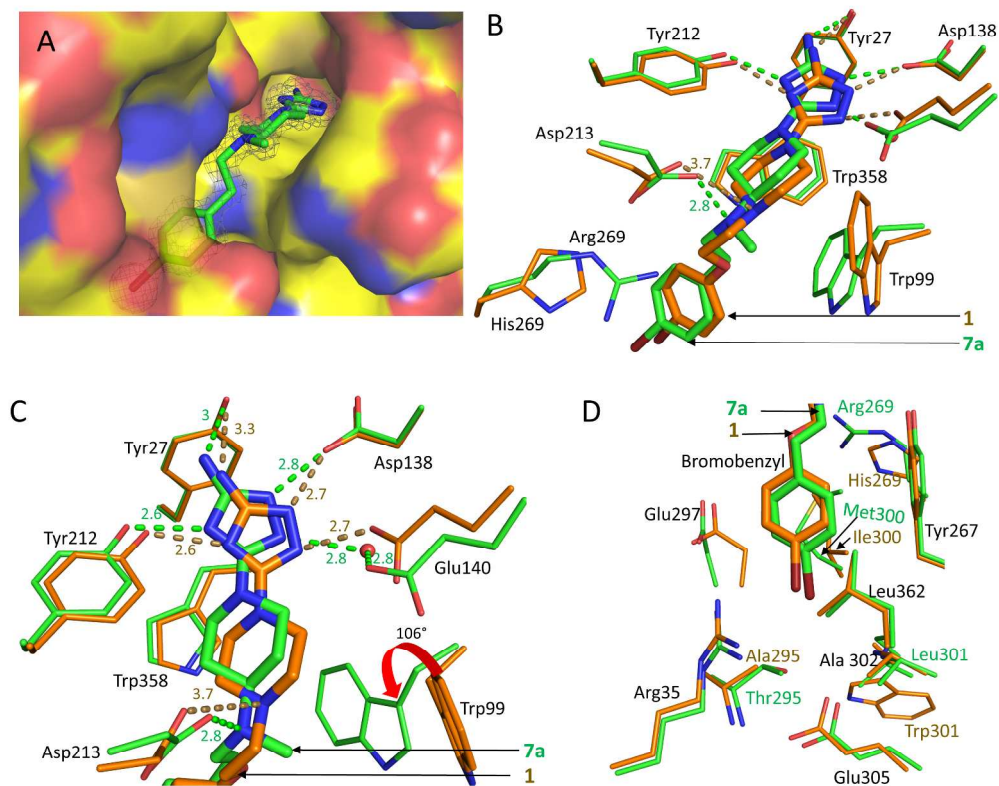


Figure 2

253x233mm (300 x 300 DPI)

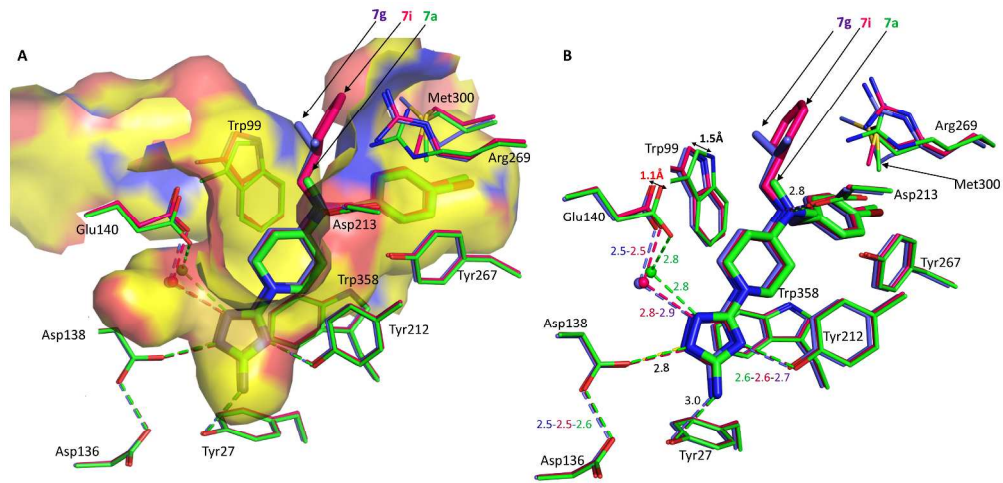


Figure 3

338x253mm (300 x 300 DPI)

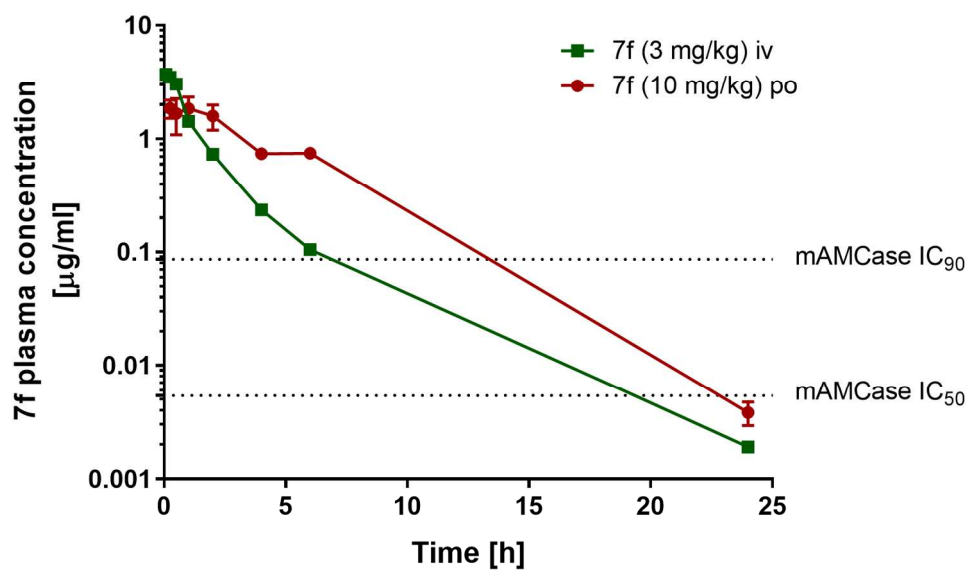


Figure 4. Plasma concentration–time course for compound 7f after 3 mg/kg iv bolus and after 10 mg/kg oral administration (po) into female BALB/c mice.

152x93mm (300 x 300 DPI)

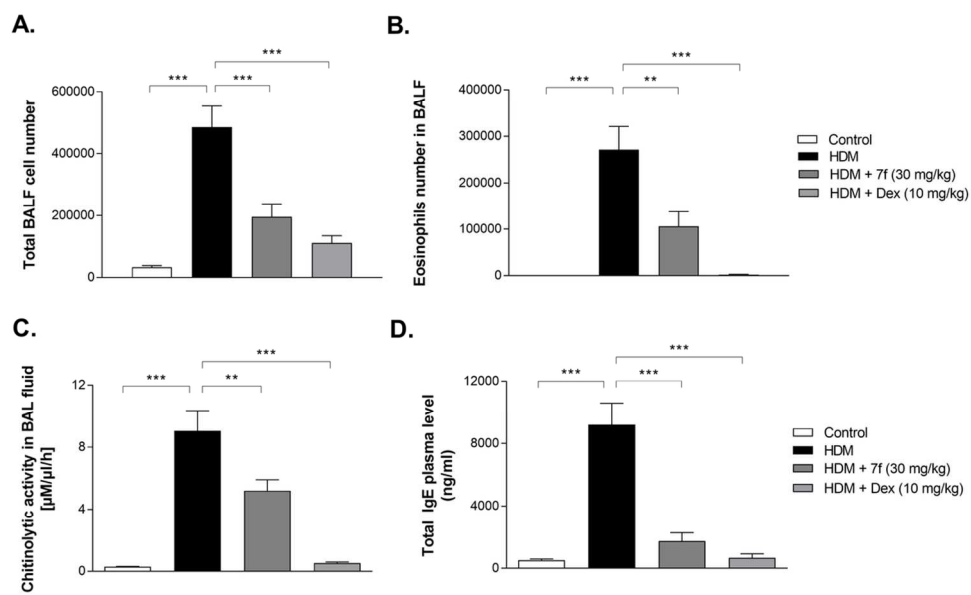


Figure 5

110x68mm (300 x 300 DPI)

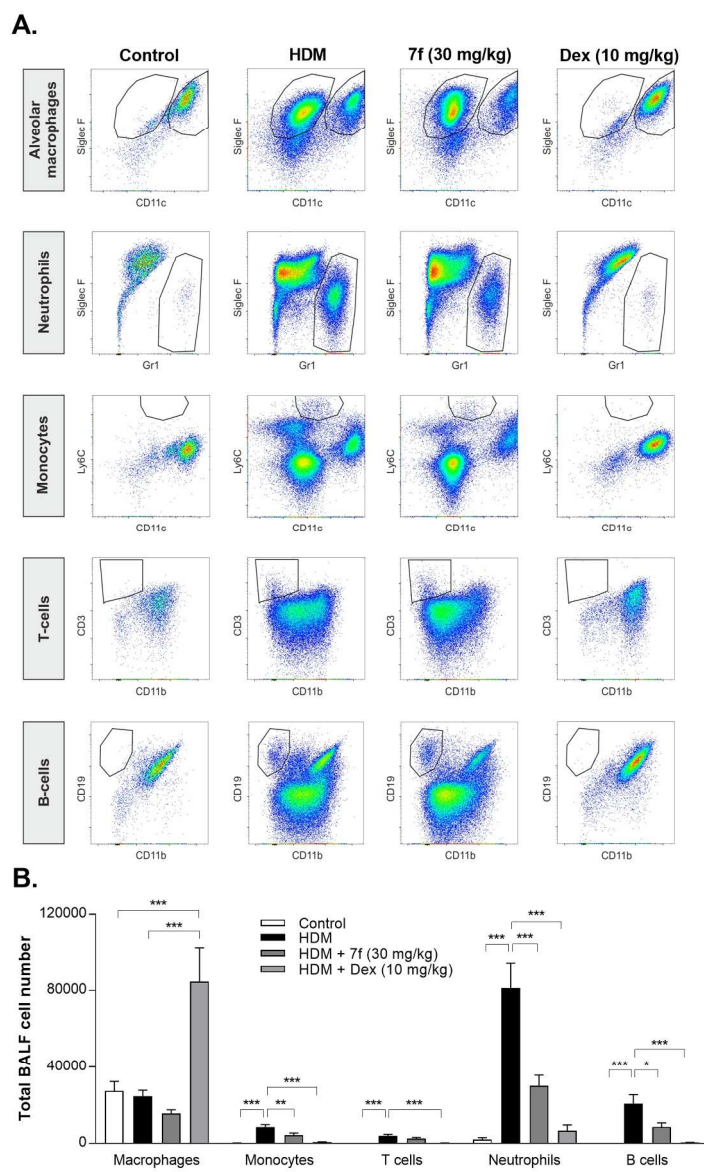


Figure 6

152x231mm (300 x 300 DPI)